Cheiron School 2011

Protein Crystallography

Macromolecular crystallography (MX)

SPring-8 / JASRI
Structural Biology Group
Takashi Kumasaka
http://bioxtal.spring8.or.jp
E-mail: kumasaka@spring8.or.jp

1

Contents

- Introduction
- Data collection method
  Experimental error, Detector
- Synchrotron beamline
  Microbeam beamline, Beamline automation,
  Remote data collection,…
- Radiation damage
  Mechanism, Cryo technique, …
- Anomalous data collection
  Optimum wavelength, Estimate signal, …

2

Introduction

3

Structural study of Ribosome

Ribosome …
plays a factory to produce protein from genetic information

Central Dogma
DNA -> RNA -> Protein

A major target of antibiotic drug

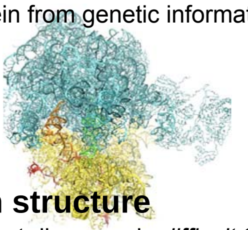

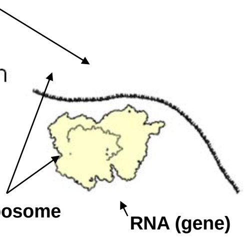

To reveal function from structure

Prof. Ada Yonath
2009 Nobel Prize

It is considered that ribosome is *difficult to be crystallized* because of its huge size. Prof. Yonath started its trial from 1980's when the other prize winners (Profs Steitz and Ramakrishnan) did not undertake it.
> Structures determined at 2000.

Used synchrotron
- ESRF ID2, ID14-2, -4, ID29
- APS 19-ID
- CHESS F1
- DESY BW6 & BW7B
- PF BL6A… and many others

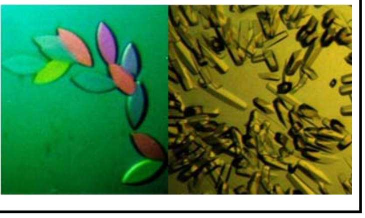

Protein structure

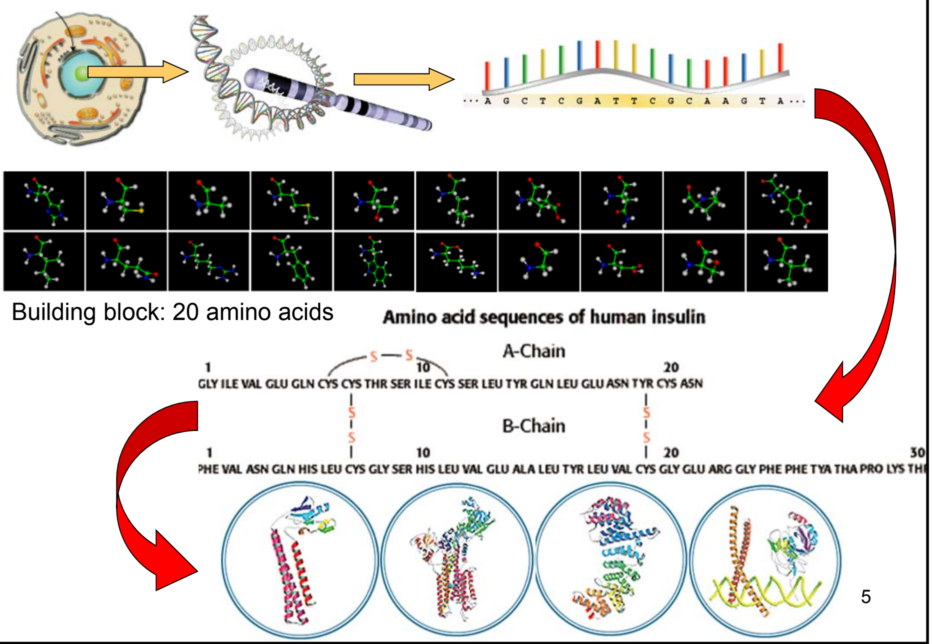

5

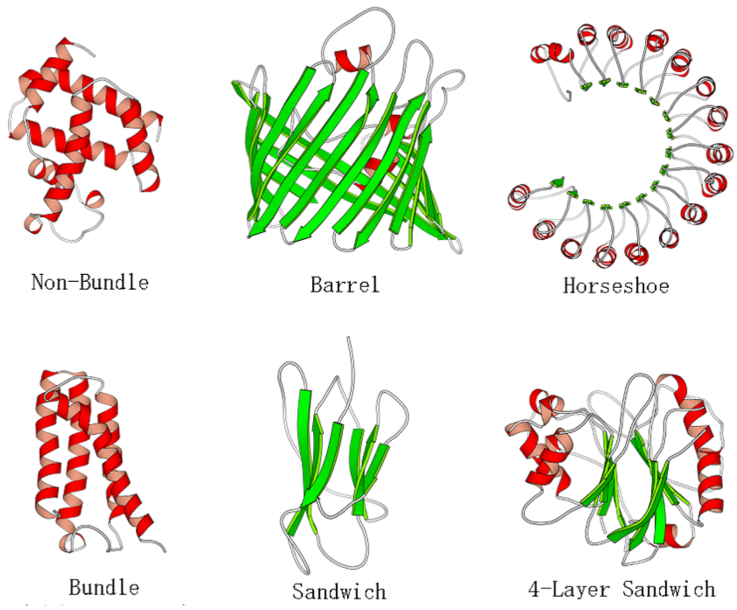

6

Application to drug discovery

Marked results

Enzyme

Reaction selectivity < Key and keyhole

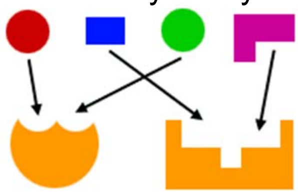

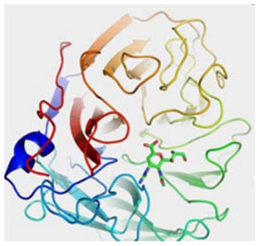

Relenza (Influenza)

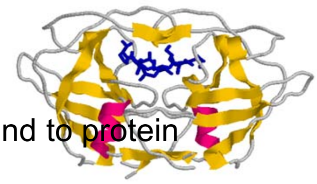

Only works a key (chemicals) can entry into the keyhole (enzyme)

Indinavir (AIDS)

Drug Design: Chemicals recognize and bind to protein structure to regulate protein function.

- **National interests and drug discovery.**
- **Keen competition in drug development.**
- **Importance structural analyses of drug-target proteins**

7

Crystal structure and synchrotron

Number of determined structures

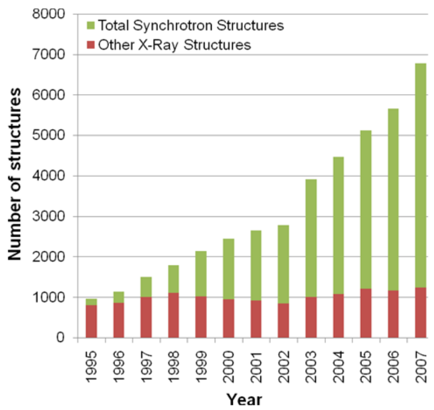

Asian contribution

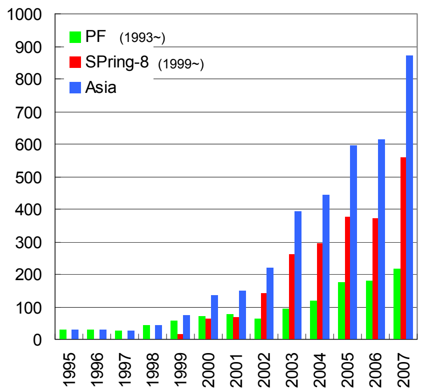

Nowadays, most structures are determined using SOR.

8

Determination of important and complex structures

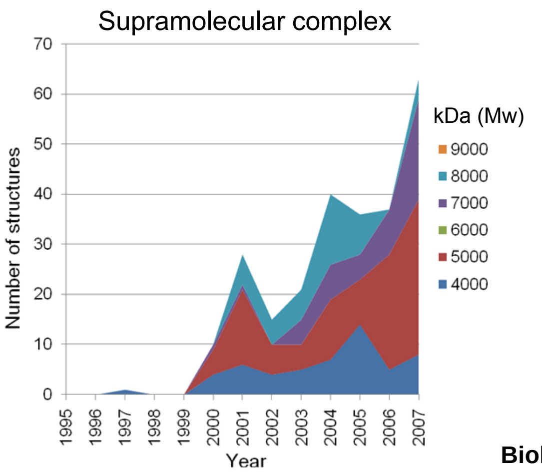

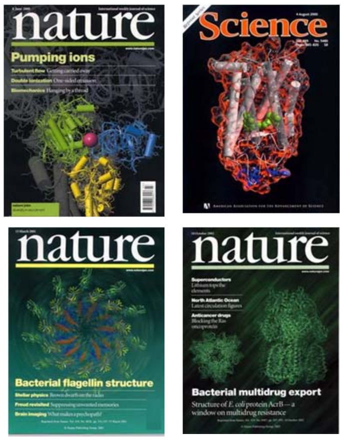

3G SOR came into this field from 2000, and accelerates large molecule analysis.

Biologically important proteins including membrane proteins: Calcium pump, Rhodopsin, Bacterial flagella, Drug effilux protein and so forth.

9

Crystal structure and synchrotron

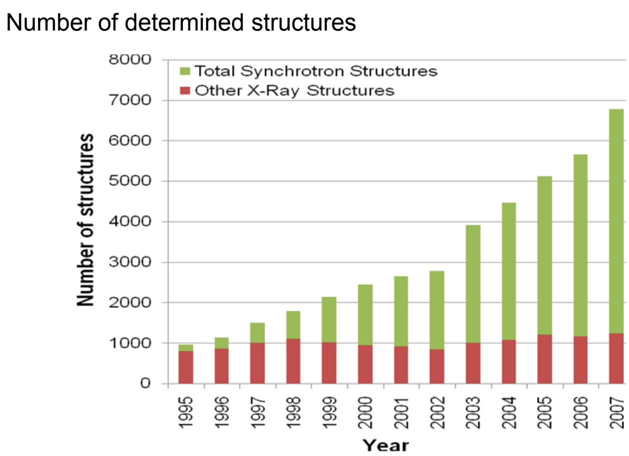

Nowadays, most structures are determined using SOR.

10

History of development in MX

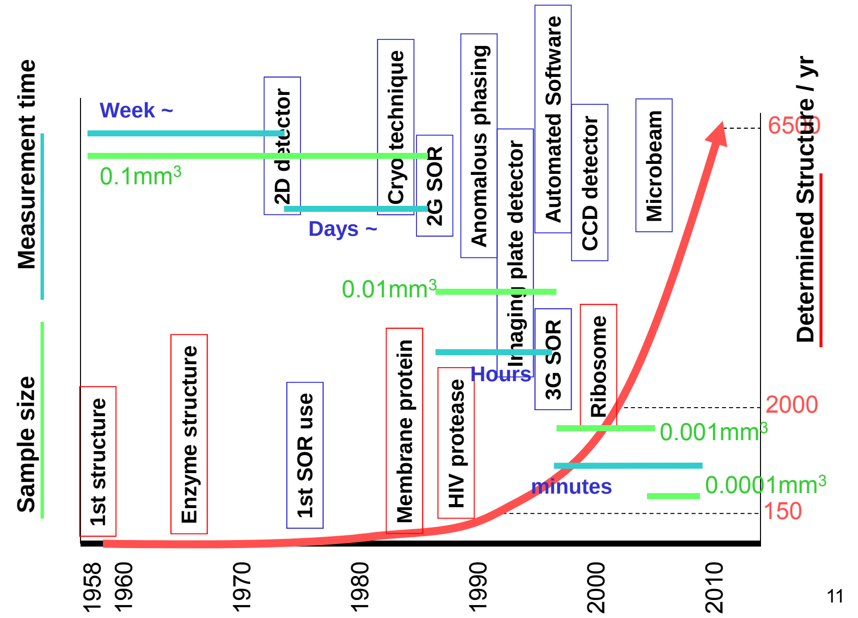

11

Advances in Protein Crystallography by Synchrotron Radiation

Steps in crystallographic analysis

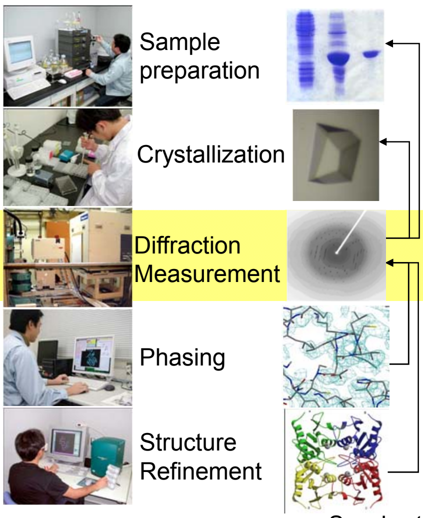

Before SOR	After SOR	3G SOR
Small amount of samples for		
10 mg~	0.1 mg~	
Small crystalline size		
0.1 mm^3~	0.01 mm^3~	0.001 mm^3~
High speed data collection		
day ~ week	**20 min ~**	**5 min ~**
New phasing method		
month ~ year	Day ~ a few months	
Automated refinement by high resolution data		
Month ~ year	Day ~ weeks	

Synchrotron data collection
> effective to not only X-ray measurement but also all other exp. steps in scale down / time reduction / high resolution.

12

Overview of data collection method
Experimental error, detector…

13

Data Collection

Real Space

$f\,(x\,y\,z)$

Atomic Scattering Factor
(Real Number)

The Principle of X-ray Crystallography

Reciprocal Space

$\boldsymbol{F}\,(h\,k\,l)$

Structure Factor
(Complex Number)

Crystal

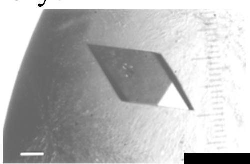

X-ray Diffraction

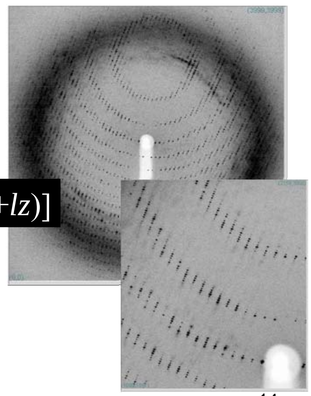

Fourier Transform

$\boldsymbol{F}(hkl) = \Sigma\, f_j \exp[2\pi i(hx+ky+lz)]$

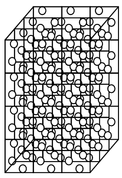

Computation

Atomic Coordinate

Diffraction Spot

14

To take good quality data sets

Essentials in high quality data collection:

Incident X-ray: Intensity, Divergence, Wavelength

Detector: Detection accuracy, Speed, Image resolution

Crystal: Crystalline order, Size, Radiation resistance

15

Experimental setup

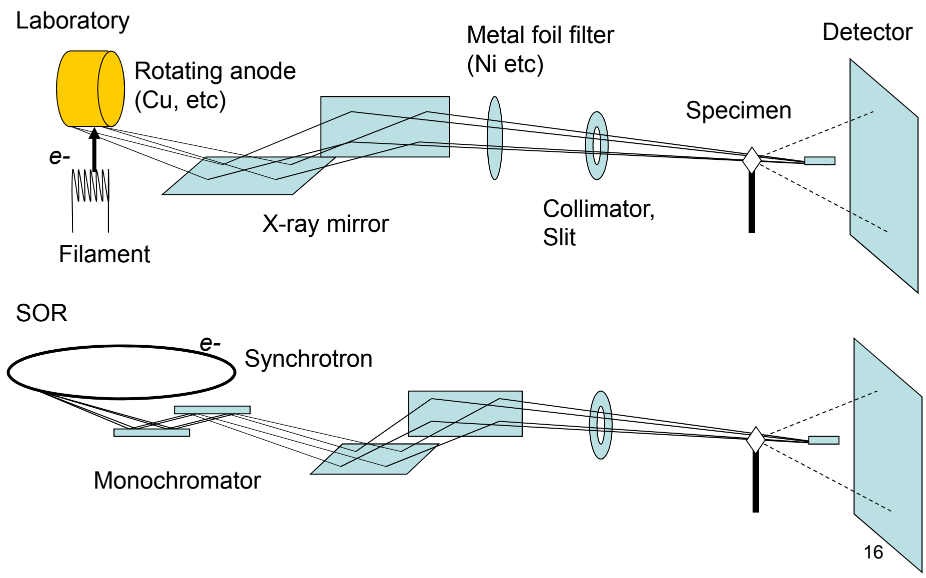

16

Parameters in oscillation method

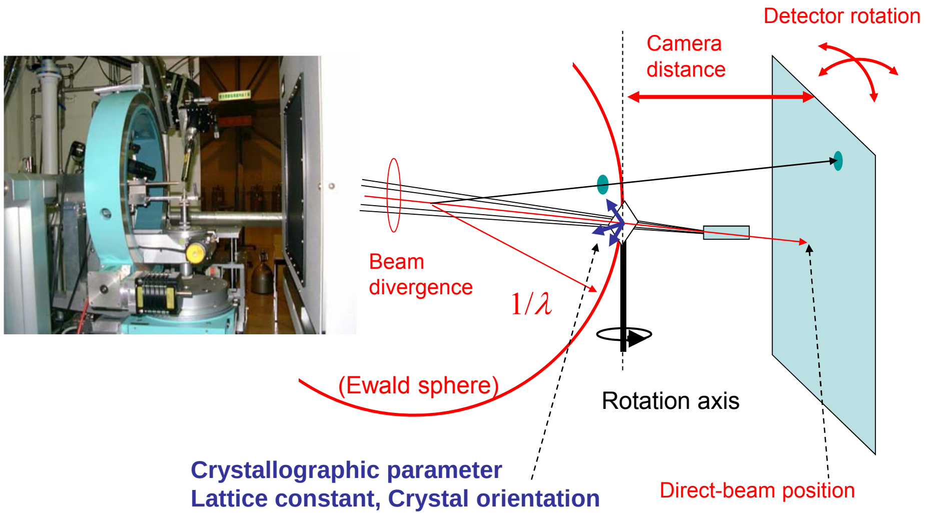

17

Signal-Noise Ratio (S/N)

Signal:	Diffraction intensity ~ Dose dependent
Noise:	Radiation damage ~ Dose dependent
	Scattering noise ~ Dose dependent
	Detector dark noise ~ Time dependent
	Detector readout noise ~ Image number dependent

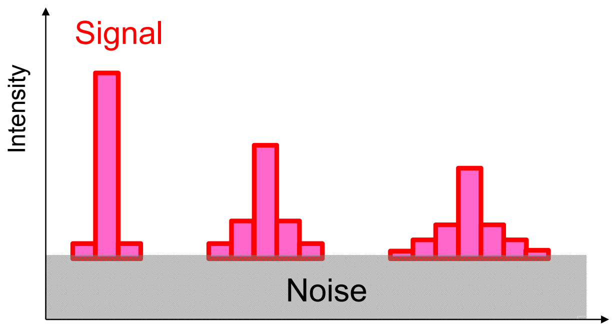

18

Mosaic spread

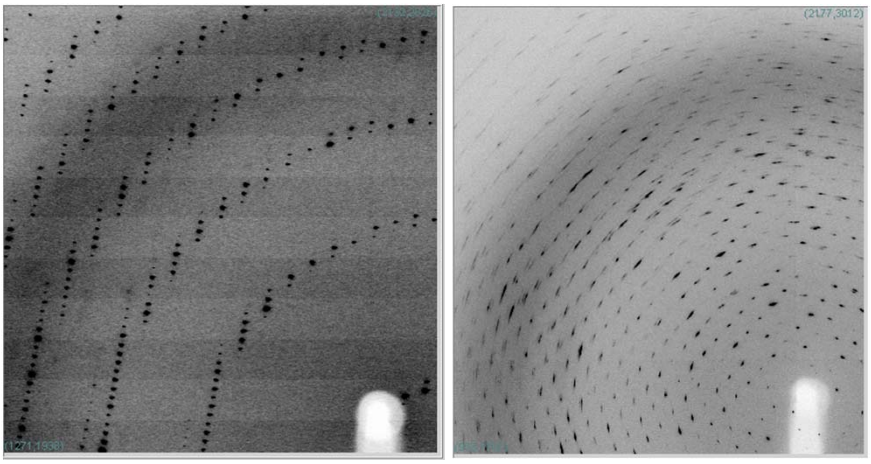

Spot sharpness depends on crystalline order.

19

Unit cell repetition & Intensity ~ Laue function

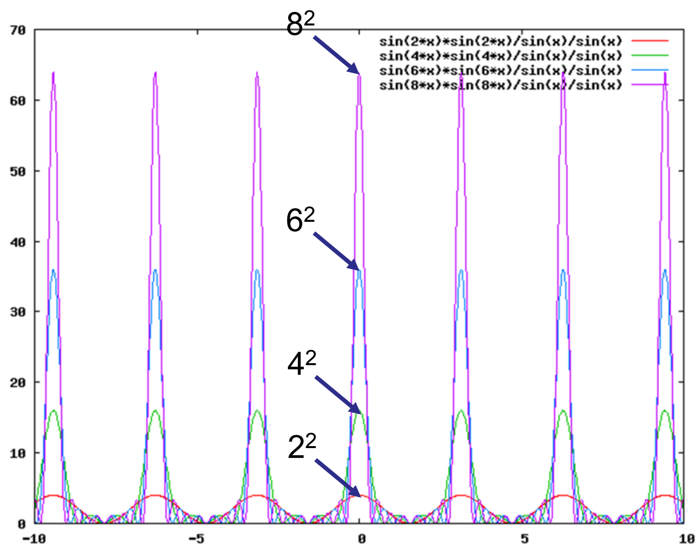

20

Cell repetition and Mosaic spread

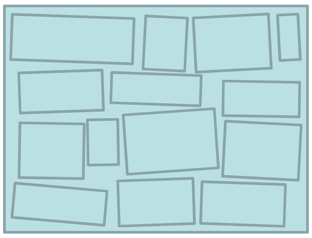

I: Peak height of a spot profile
N: number of mosaic crystals
V: average size of mosaic crystals

Half size in each dimension

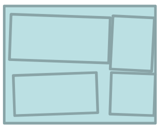

Type 1:
Small number
of mosaic crystals

$N_1 = N / (2^3)$
$V_1 = V$

$I_1 = I / (2^3)$

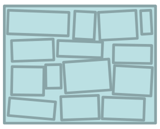

Type 2:
Small size
of mosaic crystals

$N_2 = N$
$V_2 = V / (2^3)$

$I_2 = I / (2^{2*3})$

21

Diffraction power of crystal

Darwin's Formula

$$E(\mathbf{h}) = \frac{I_0}{\omega} \lambda^3 \frac{e^4}{m^2 c^4} \frac{P \cdot L \cdot A \cdot V_x}{V^2} \cdot \left| F(\mathbf{h}) \right|^2 \cdots$$

I_0: Incident intensity, ω: Angular velocity of crystal rotation, λ: Wavelength,
e: Charge of electron, P: Polarization factor (= $(1+\cos^2 2\theta)/2$),
L: Lotentz factor (= $1/\sin\theta$ when spindle x-ray),
A: Absorption coefficient, V_x: Crystal volume, V: Lattice volume

In case of protein crystal…

- High solvent contents (25 ~ 75%)
- Large unit cell

> Weak diffraction power ~ Low resolution

22

Crystal packing ~ molecular vibration ~ resolution

Relationship with B-factor (DWF)

Vibration in solution > Movie

Packing density V_M:

$V_M = V_{cell} / Mw_{cell}$

High density (small V_M) > High Rigidity

(Kantardjieff & Rupp, 2003)

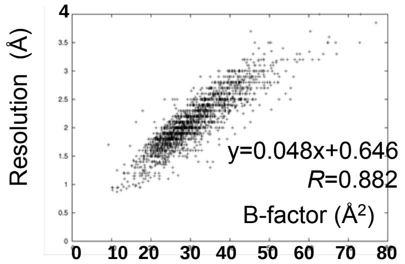

Packing control by humidity control

FMS (Free Mounting System)

> lower humidity around crystal

> dehydration

> induce phase transition

(Kiefersauer et al., 2000)

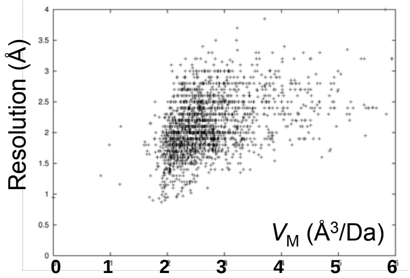

Relative Wilson statistics and intensity

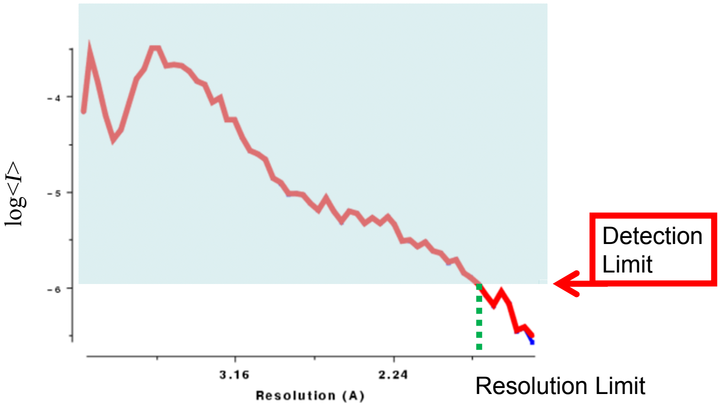

$$d^{*2} = 4\sin^2\theta/\lambda^2$$

24

Resolution and incident intensity

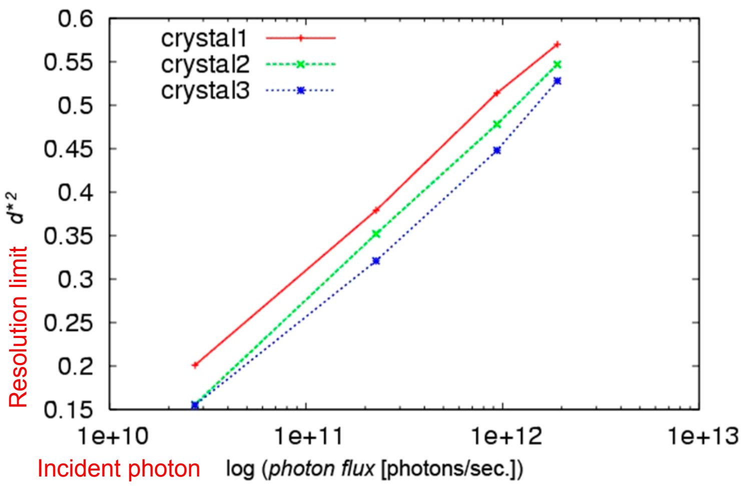

K. Hirata (RIKEN), Personal communication 25

Diffraction power reduction by radiation damage

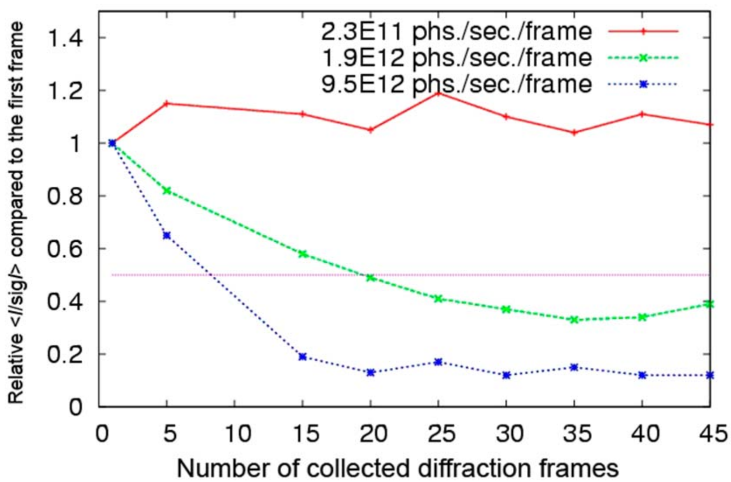

K. Hirata (RIKEN), Personal communication 26

2D detectors for MX

	CMOS	CCD Indirect	CCD Direct	Amorphous Selenium	Silicon Pixel	IP
Area size (100-400mm)	○ Multi-element	○ ME+FOT	△ cm sq. order	◎ by processing tech.	○ ME	◎
Resolution (50-100μm)	◎ Few-200 μm Phosphor	○ 10 - 100 μm FOT&phosphor	◎ Few μm	○ 100~200 μm	△ ~200 μm	○ 50 μm~
Readout Speed	◎ Sub mSec Continuous readout	○ Sec		○ Sec	◎ Real time Counting	△ Min
Sensitivity	△~◎ Phosphor & Window	△~◎ Phosphor		△	△~◎ Low for high E photon	◎
Noise	△~○ Relatively high readout & dark noise	○ Successful Cooling Phosphor/FOT/Window		△ Higher noise by polycrystalline	◎ Counting (counting loss at high dose)	△ Stray light of laser / Loss of fluorescence Capture
Skew	◎	△ FOT	◎ Direct	◎ Direct	◎ Direct	○~◎ Geometry at readout
Dynamic range	△ ~12bit	○ ~16 bit		○ ~16 bit	◎ ∞ (Counting)	◎ ~20 bit
Cost	◎ Versatile Processing technology	△~○ Complex system	◎ Cheap but small	? Expecting Future development	△ Original tech. and monopolistic	◎ Simple and matured technology

27

Imaging plate

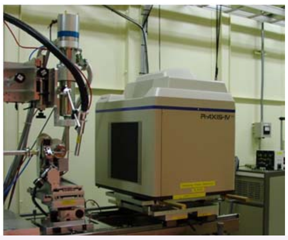

Plastic X-ray sensitive film
Photostimulated luminescence by $BaFBr:Eu^{2+}$

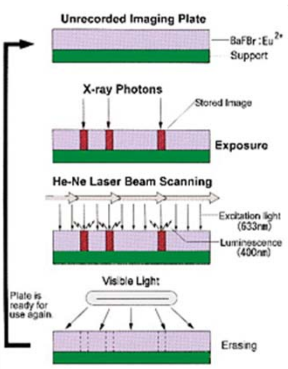

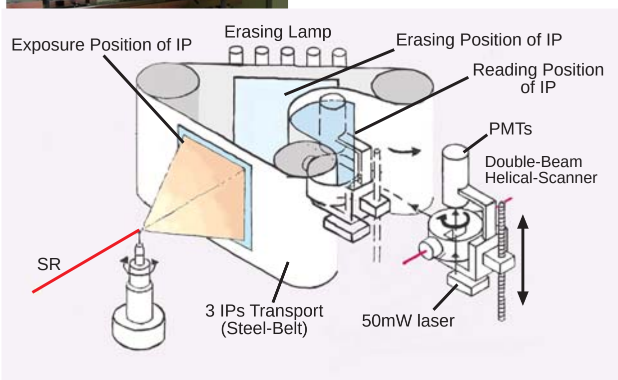

(Rigaku, Japan) 28

CCD Detector

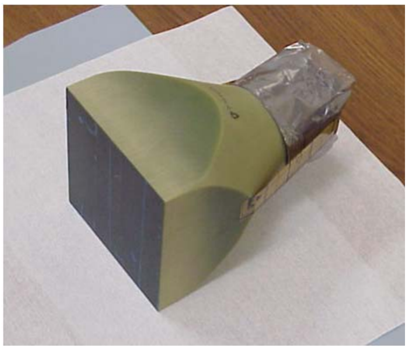

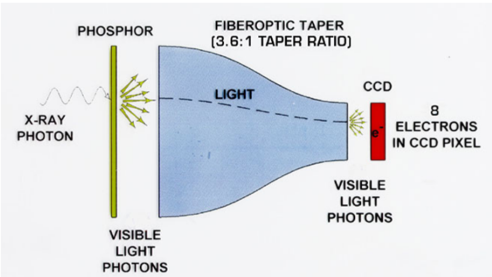

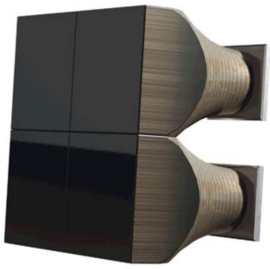

29

CCD detector system

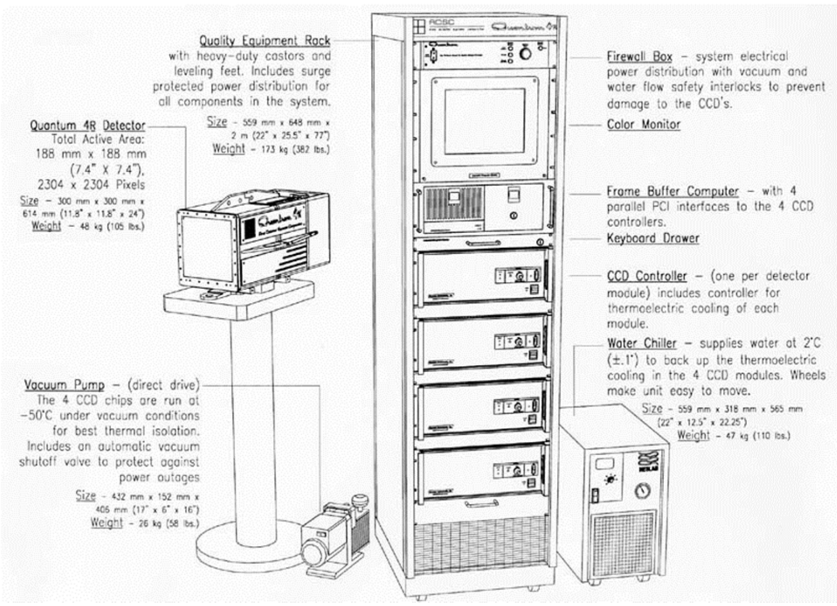

Area Detector Systems Co. http://www.adsc-xray.com

Silicon pixel detector

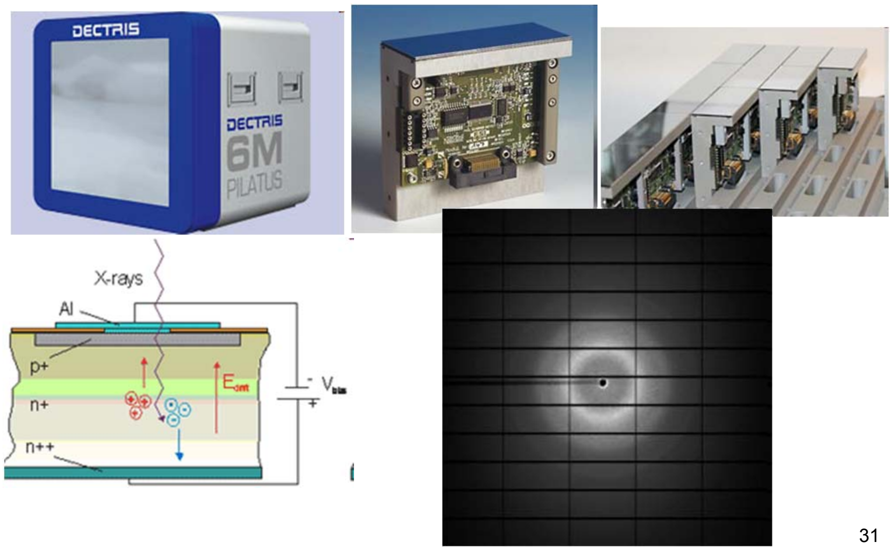

31

Dectris: http://dectris.com/

Continuous rotation data collection by CMOS Detector

Hasegawa (JASRI) &
Yamamoto (RIKEN) et al.
Hamamatsu Photonics

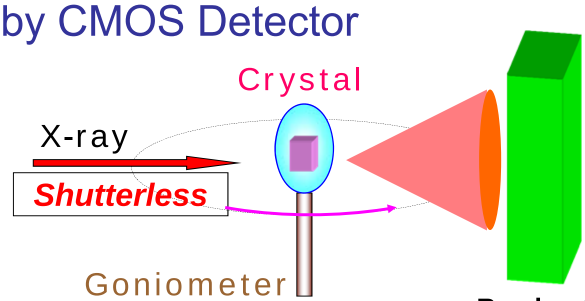

Rotate with a constant speed

Read out images with a constant frame rate

High throughput and/or Fine slice data collection

Specification	Hamamatsu C10158DK	ADSC Q210
Scintillator	CsI:Tl	Gd_2O_2S:Tb
Pixel size [mm^2]	50 x 50	51 x 51
Detector area [mm^2]	118.8 x 118.8	210 x 210
Output data [bits]	14	16
Dynamic range	6,000	14,100
Dead time due to readout	14 msec / pixel	1.1 sec / frame

32

Synchrotron Beamline

33

3: Recent advances in MX beamlines

MX Beamlines at SPring-8

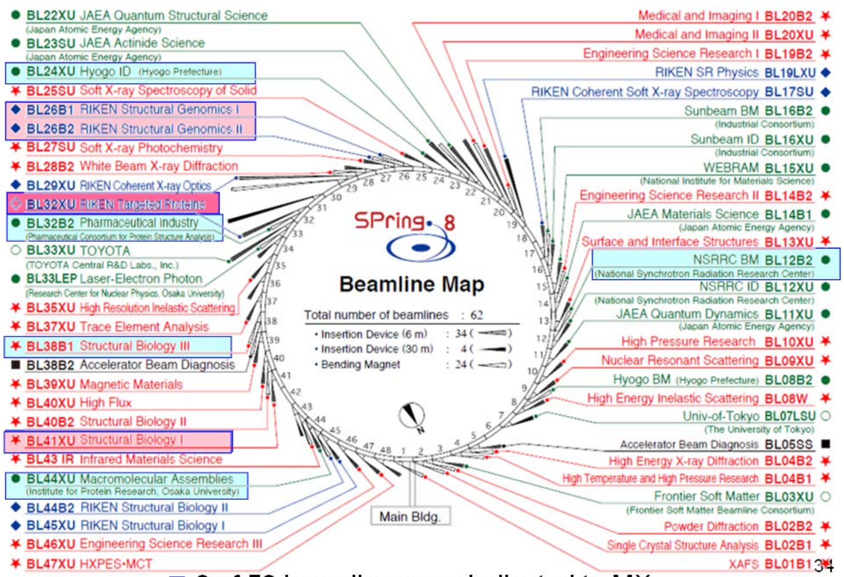

■ 9 of 53 beamlines are dedicated to MX

34

Beamlines and User Accessibility

1. Public Beamlines (BL41XU, BL38B1; JASRI)
   Academic use + Proprietary use (incl. Mail-in service)

2. Contract Beamline (BL44XU; Osaka Univ.)
   Academic use

   Contract Beamline (BL24XU; Hyogo Pref.)
   Academic use + Partially opened to proprietary use

3. RIKEN Beamlines (BL26B1&B2, BL32XU; RIKEN)
   RIKEN's academic research + Partially opened to public use (20%)

4. Pharmaceutical Industrial Beamline (BL32B2; PcProt)
   Fully operated for propietary use
   by the members of
   Japan Pharmaceutical Manufacturers Association (JPMA)

35

Synchrotron MX

Brilliant synchrotron radiation facilitates MX research

1. For cutting edge research
   High precision data collection
   for Micro-crystal & Large unit-cell samples

2. For structural genomics approach
   Automated and rapid data collection
   for High throughput screening

36

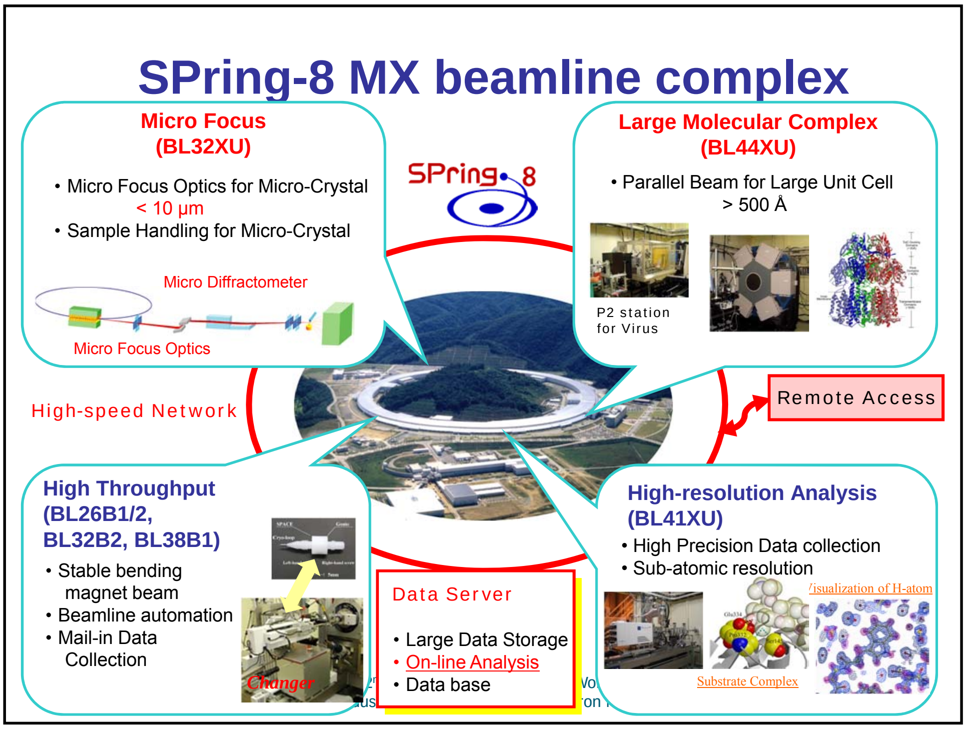
SPring-8 MX beamline complex
Micro Focus
(BL32XU)
• Micro Focus Optics for Micro-Crystal
< 10 µm
• Sample Handling for Micro-Crystal
Micro Diffractometer
Micro Focus Optics
SPring-8
Large Molecular Complex
(BL44XU)
• Parallel Beam for Large Unit Cell
> 500 Å
P2 station
for Virus
High-speed Network
Remote Access
High Throughput
(BL26B1/2,
BL32B2, BL38B1)
• Stable bending
magnet beam
• Beamline automation
• Mail-in Data
Collection
Changer
Data Server
• Large Data Storage
• On-line Analysis
• Data base
High-resolution Analysis
(BL41XU)
• High Precision Data collection
• Sub-atomic resolution
Substrate Complex

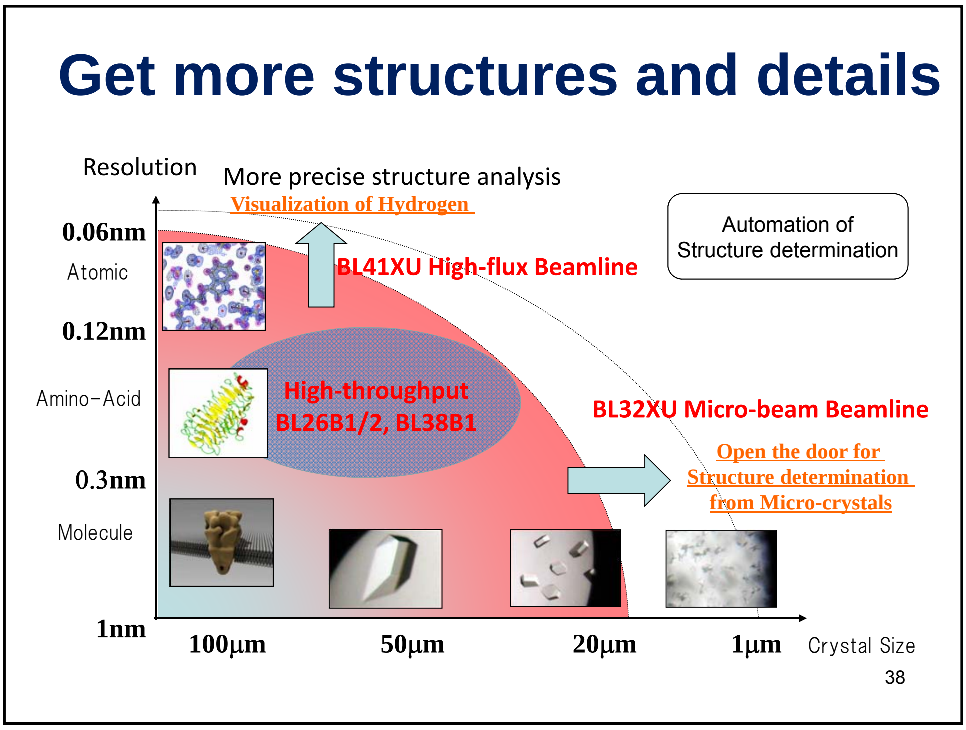
Get more structures and details
Resolution
More precise structure analysis
Visualization of Hydrogen
Automation of
Structure determination
0.06nm
Atomic
BL41XU High-flux Beamline
0.12nm
Amino-Acid
High-throughput
BL26B1/2, BL38B1
BL32XU Micro-beam Beamline
Open the door for
Structure determination
from Micro-crystals
0.3nm
Molecule
1nm
100µm
50µm
20µm
1µm
Crystal Size
38

Development of micro-beam beamline

X-ray crystallography of proteins related to human disease and aging.

Micro-beam optimized for Micro-crystal

Standard	Current Limit	Micro-crystal
>50μm	20~30μm	<10μm

Target Crystals

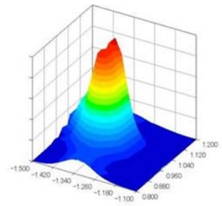

Beam profile of SPring-8 BL41XU

	Current	Target Beam Size	
• Beam Size	30×30	1×1	μm²
• Flux density	10^9	$>10^{10}$	photons/sec./μm²

39

R&D target for Micro-crystallography

Micro-crystal
- **Small size crystal（<10mm）**
- **Weak signal（10^6copies）**

Maximize signal-to-noise ratio
- **Generate micro-beam**
- **Optimize experimental equipments**

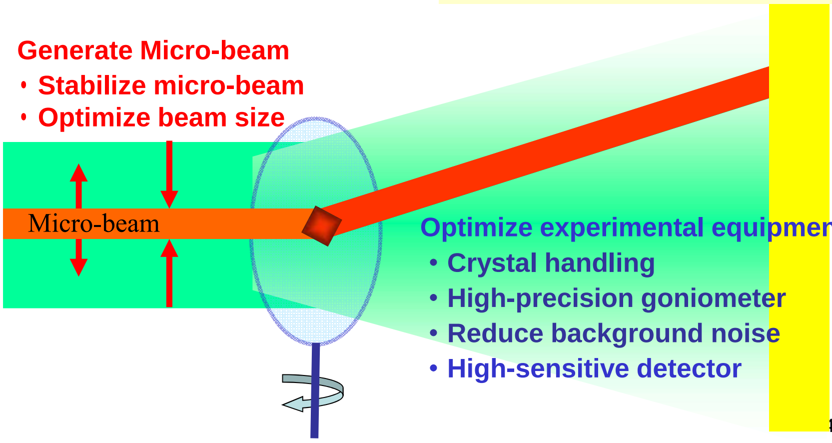

40

Design concept of BL32XU

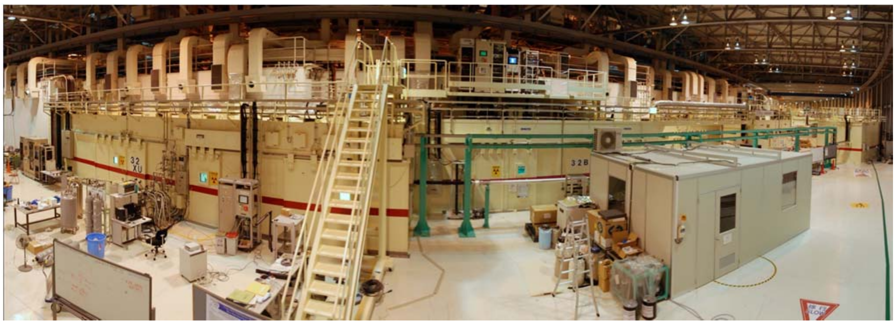

1. Brilliant source
2. Simple components
3. Focusing X-rays with large magnification factor
4. Changeable beam size at sample position

41

K. Hirata, M. Yamamoto (RIKEN) et al.

Beamline components

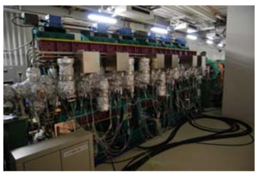

Hybrid in-vacuum undulator

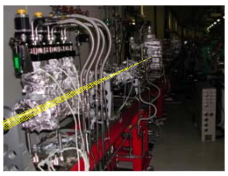

Front end

High precision double crystal monochromator

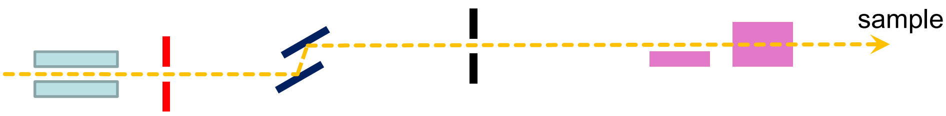

K-B focusing mirrors

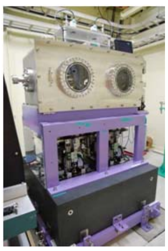

Co-axial sample camera

High precision goniometer

High efficient CCD detector

EEM-mirrors for 1 um focusing

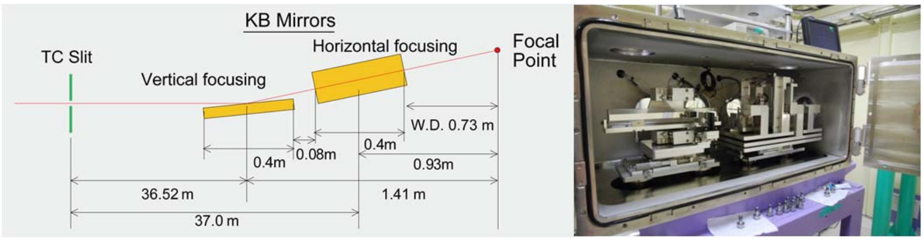

Designed mirror surface shape

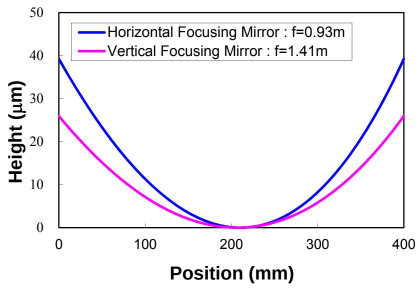

Kirkpatrick-Baez Mirror

Mirror shape :	Elliptical
Mirror length :	400 mm
Energy range :	8-20 keV
Mirror material :	SiO_2
Mirror surface :	Pt-coated
Glancing angle :	3.5mrad

43

Design of focusing optics

- Virtual light source is TC-Slit (located at 36m upstream of 1st mirror)
- Pt-coated elliptical mirrors with K-B (Kirkpatrick-Baez) configuration
- Magnification factors: 26 in vertical, 40 in horizontal
- Beam divergence at sample position < 2 mrad
- Available X-ray energy range: 8 - 20 keV, especially high-flux at 12.4 -13.8keV

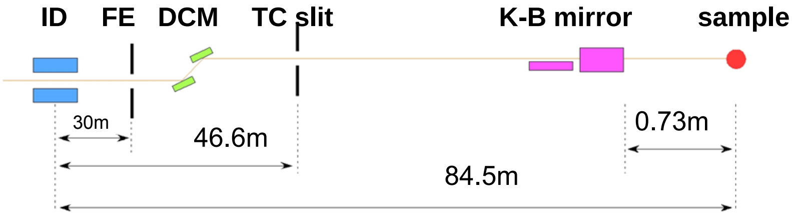

Beam size @ sample	1(H) x 1(V) μm^2	20(H) x 19(V) μm^2
TC slit size	40(H) x 26(V) μm^2	800(H) x 500(V) μm^2
Photon flux@12.4 keV	**6 x 10^{10} photons/s**	2 x 10^{13} photons/s

Glancing angle is designed at 3.5mrad

44

Achieved beam size（2009/11/27）

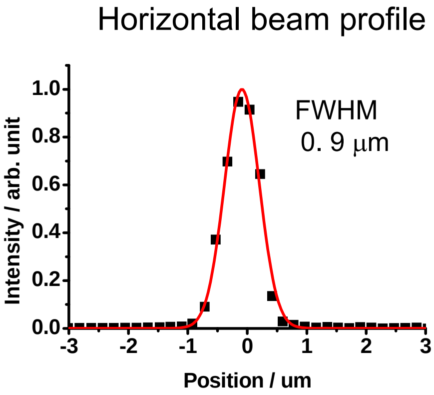

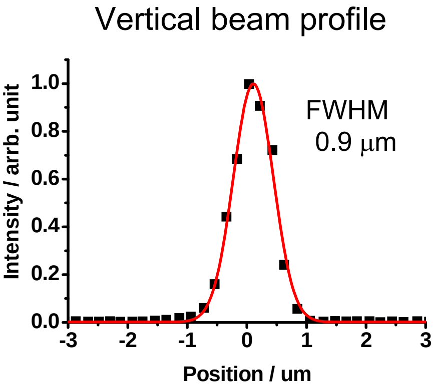

Focused photon flux : 6.2×10^{10} photons/sec

The smallest & highest flux density in the world

45

Micro-crystal diffractometer

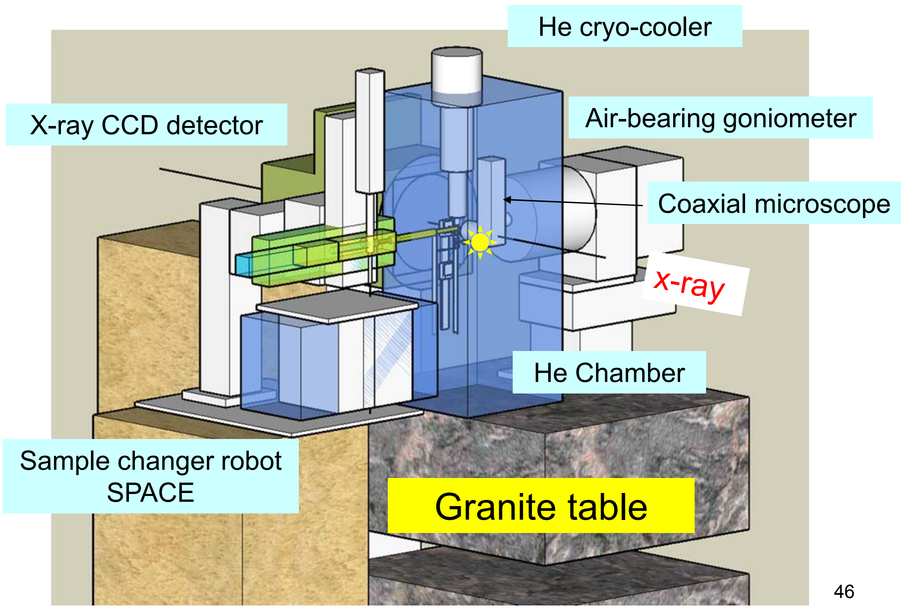

46

Air-bearing goniometer

- High-precision spindle axis with air-bearing unit
- Hi-speed rotation useful for fast centering, inverse beam geometry etc.

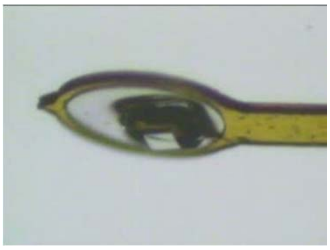

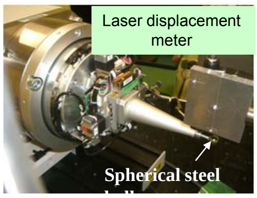

Eccentricity < 0.7μm/360°

(KOHZU PRECISION Co., LTD.)

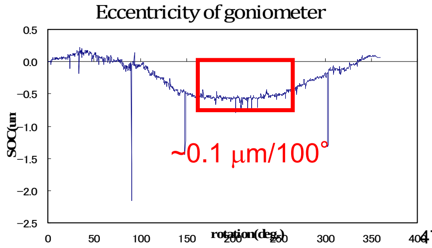

47

Tentative diffractometer setting

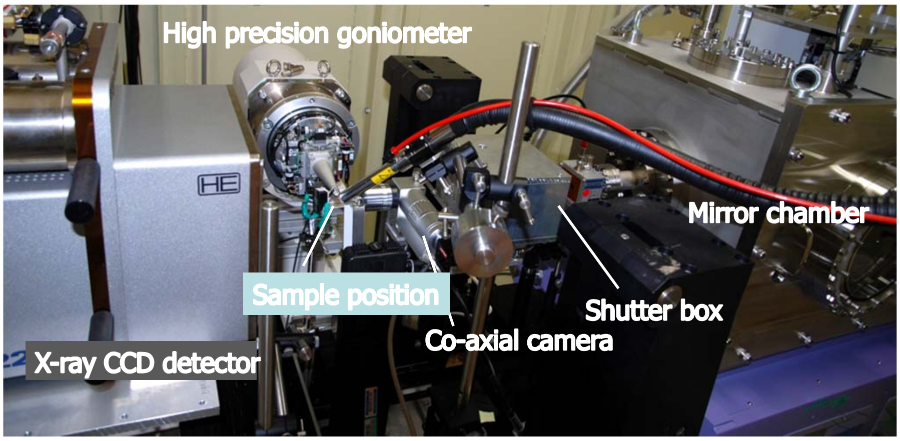

Focusing mirror -> Ion chamber -> Shutter -> Co-axial sample camera -> Collimator -> Back light -> Beam stopper

48

The first crystal onto the 1μm beam

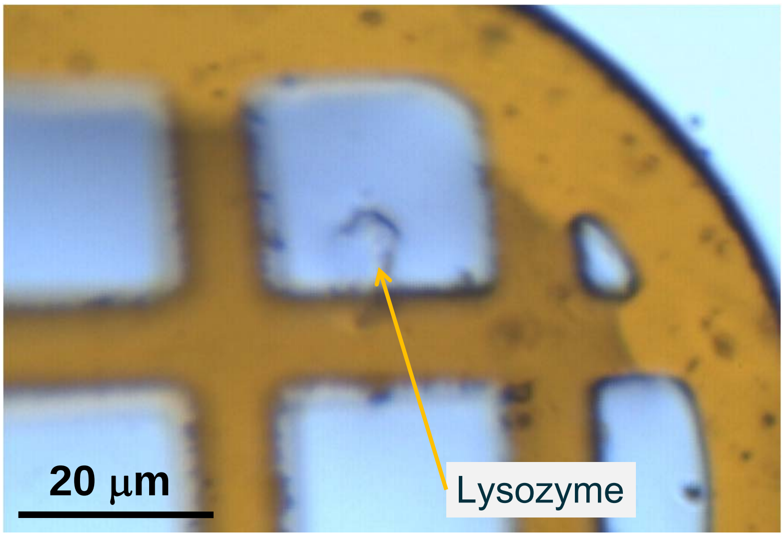

49

The first diffraction image (09/12/04)

Crystal	Lysozyme 5um crystal
Beam property	1mm square, 2.6×10^{10} photons/sec.
Exposure time	1 sec.
Resolution limit	2.0 Å

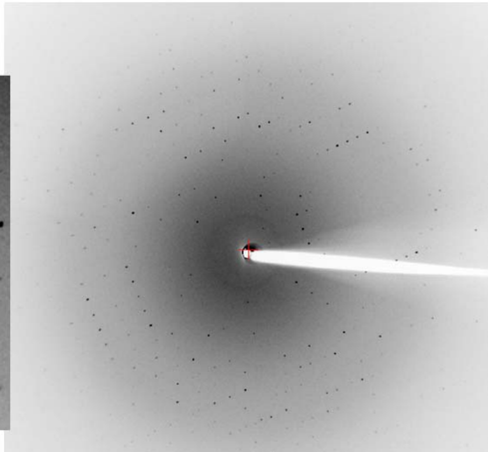

Larger beam divergence did not badly affect diffraction profiles

Data collection limit by crystal size

Acta Cryst. (2008), D64, 158-166

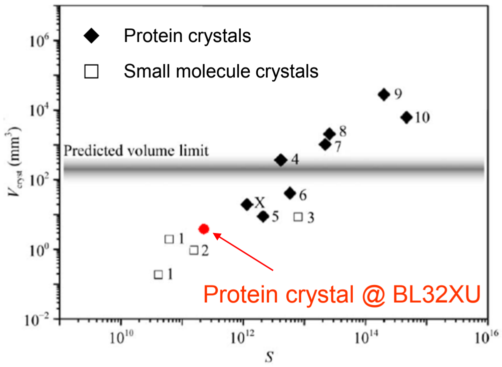

Formula of diffraction power

$$S = (F_{000} / V_{cell})^2 \times \lambda^3 \times V_{cryst}$$

We collect a 2 Å resolution data from 2 um lysozyme crystal.

BL32XU open the new field of Protein micro-crystallography

51

A recent result of a structure determination

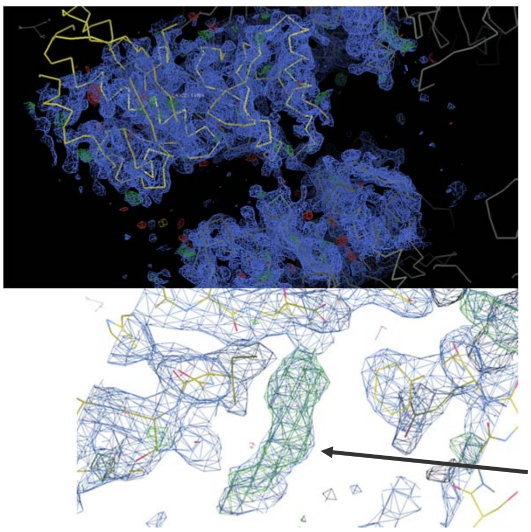

2.6 Å *C*222$_1$,
1 degree x 90 images,
from a single crystal
(0.015 x 0.012 x 0.012 mm).
1μm beam, 1 sec exposures

Completeness=96.5%
(93.9%, 2.69-2.6A)

Apr. 2010

Drs. Sengoku and Bessho
(RIKEN)

Extra electron density
of a drug candidate.

52

BL Automation

Samples & data management

D-Cha (Database for Crystallography with Home-lab. Arrangement)
Crystal information database, Schedule editor, Image browser, etc. on the Internet

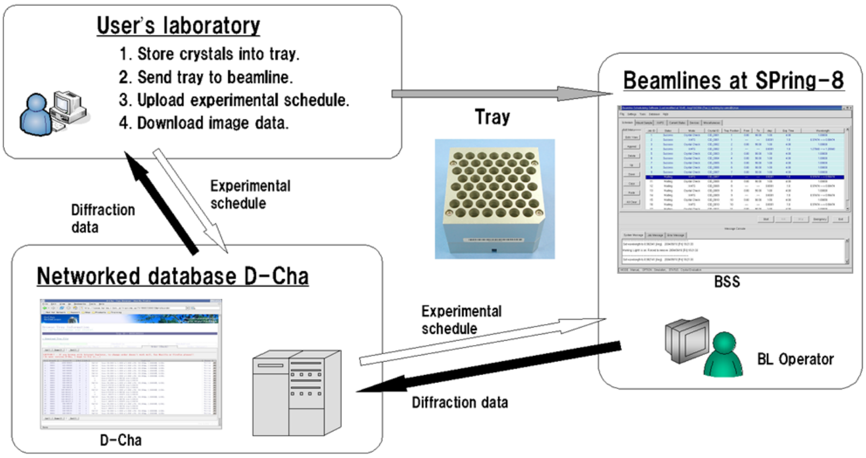

SPACE *SPring-8 Precise Automatic Cryo-sample Exchanger*

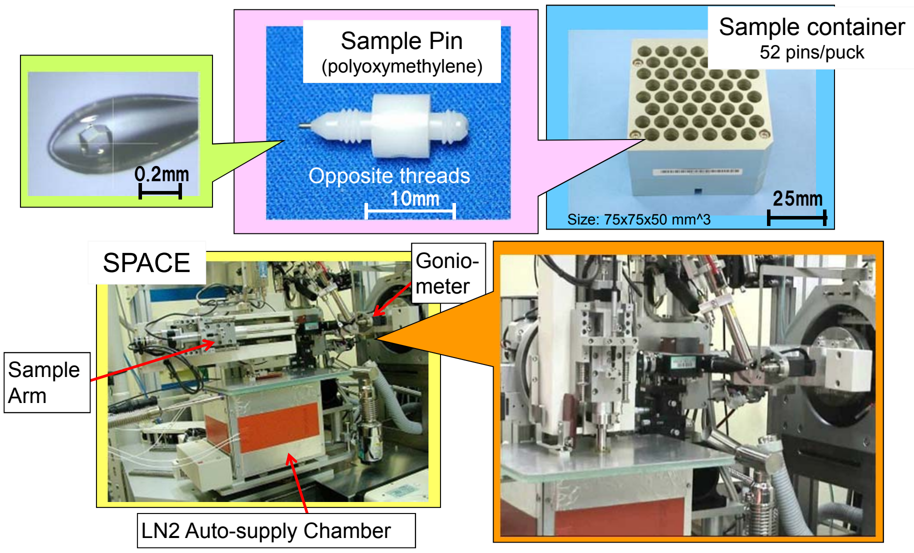

54

Ueno, Kanda, Ida, Kumasaka, Yamamoto (RIKEN) et al.

New attachment for Hampton/SPINE pins with Unipuck and other flat type cassettes

Hampton pin SPINE pin

from Robo-Sync web

(Murakami, Ueno, Yamamoto et al., Patent #2009-115652)

55

Remote Access
Convenient use without visitation

Automation of beamline control

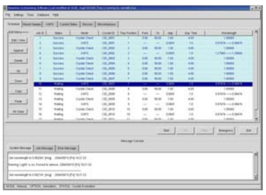

Beamline control software BSS

- Integrated control of beamline optics and diffractometer.
- Automatic set-up of measurement condition.
- Multiple measurements proceed in the scheduled order.

Automation of sample mounting

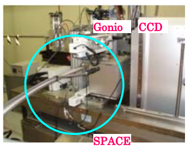

Sample changer SPACE

- Mount specimens on goniometer instead of users.
- Combination of BSS & SPACE enables automatic data collection with exchanging crystals.

Mail-in data collection

- Send crystal to SPring-8
- Edit measurement condition with D-Cha
- Collect data with a help of BL operator

Beamline database D-Cha

Sharing information between users' lab & SPring-8

- Crystal related information
- Measurement condition & schedule
- Recorded images

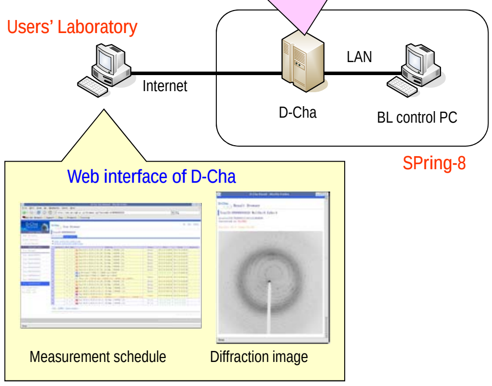

56

Remote access at SPring-8 MX beamlines

<u>Basic concept</u>

Make use of sample changer SPACE, integrated beamline control software *BSS* and beamline database *D-Cha* to make all operations required in MX data collection from remote env.

<u>Characteristic features of remote access at SPring-8</u>

- Spec fulfilling the strict radiation safety regulation in Japan
  - Not use the NX client for secure access to BL inside gateway.
  - Remote client & local server architecture with the original protocol.
  - Authentication gateway and operation restricts units are installed between the client-server to ensure safety of remote access.
- New original protocol developed as a SPring-8 standard
  For the future use other than MX BL…
  <u>Remote access composed of three session (network connection)</u>
  1. Streaming session
  2. Device control session <<<
  3. Result view session

Hasegawa, Ueno, Furukawa et al. (2010)

57

Streaming session

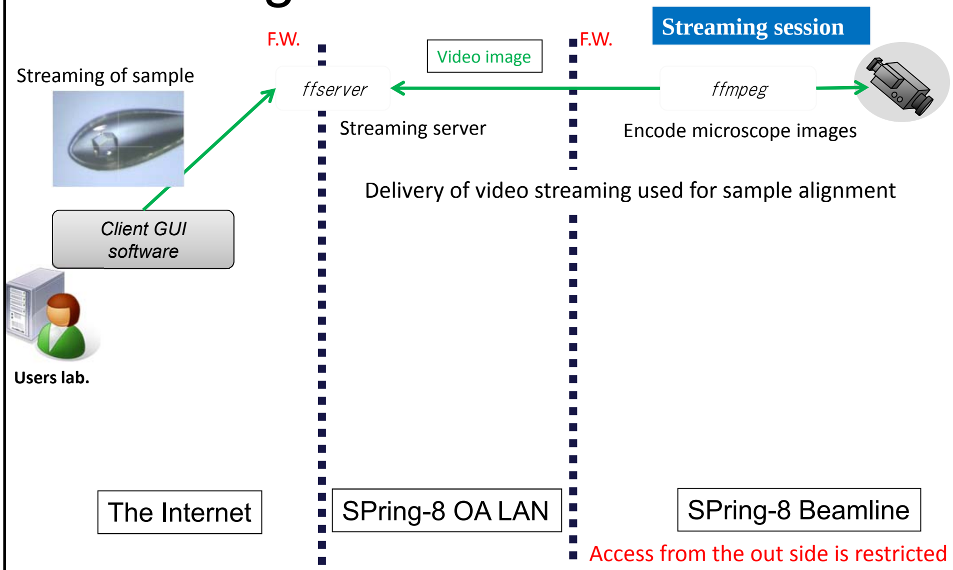

58

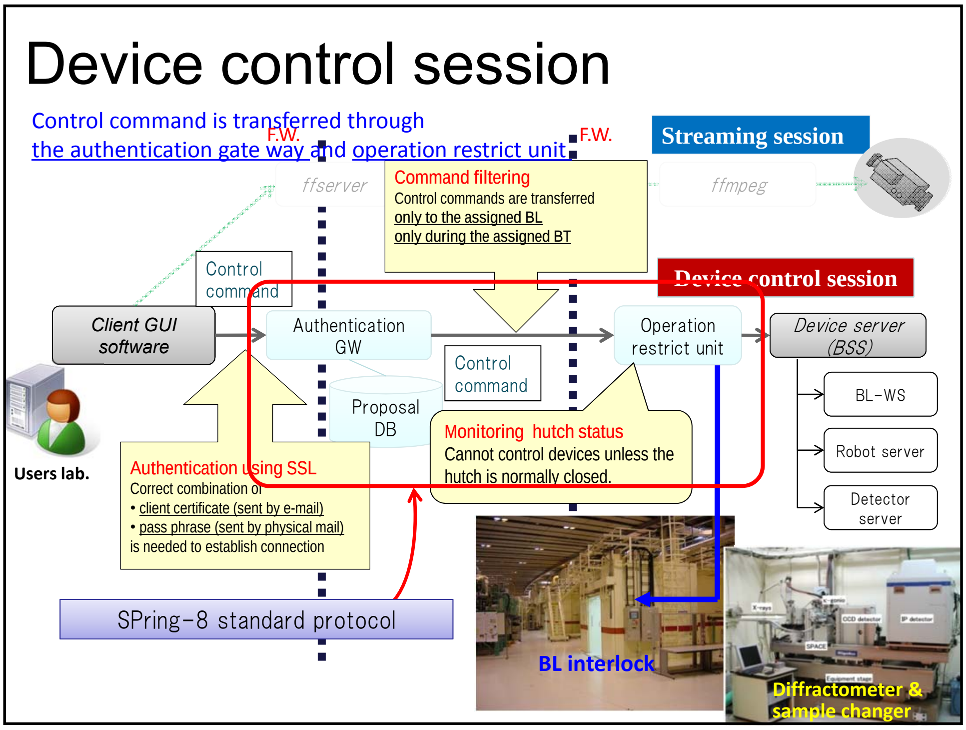
Device control session
Control command is transferred through
the authentication gate way and operation restrict unit
F.W.
F.W.
Streaming session
ffserver
ffmpeg
Command filtering
Control commands are transferred
only to the assigned BL
only during the assigned BT
Control command
Device control session
Client GUI software
Authentication GW
Operation restrict unit
Device server (BSS)
Control command
Proposal DB
BL-WS
Robot server
Detector server
Users lab.
Monitoring hutch status
Cannot control devices unless the hutch is normally closed.
Authentication using SSL
Correct combination of
• client certificate (sent by e-mail)
• pass phrase (sent by physical mail)
is needed to establish connection
SPring-8 standard protocol
BL interlock
Diffractometer & sample changer

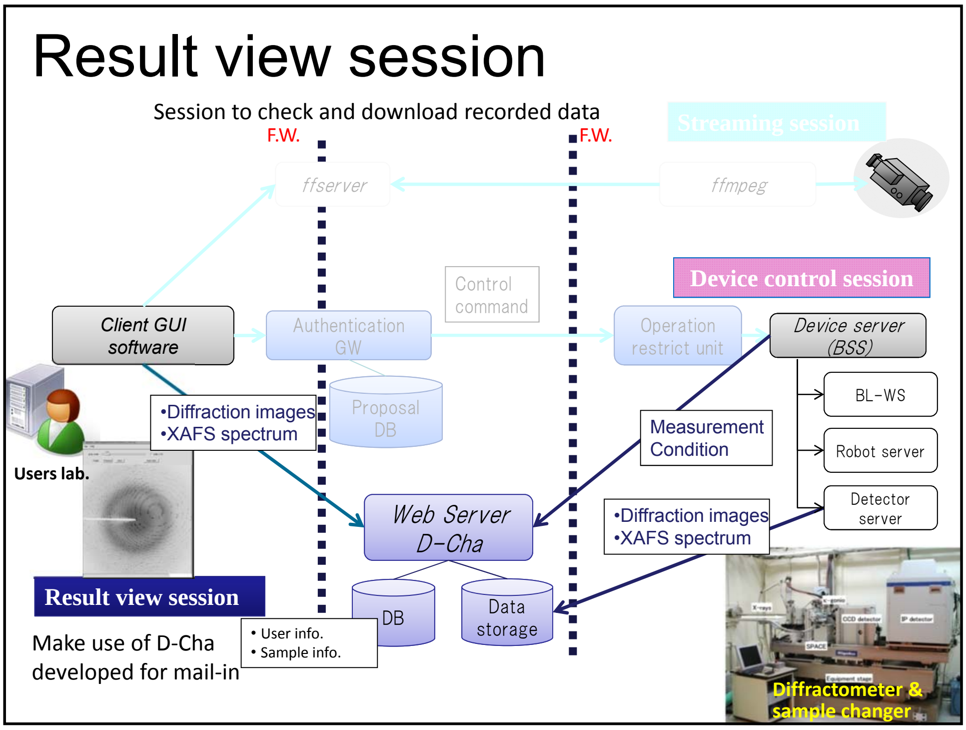
Result view session
Session to check and download recorded data
F.W.
F.W.
Streaming session
ffserver
ffmpeg
Control command
Device control session
Client GUI software
Authentication GW
Operation restrict unit
Device server (BSS)
BL-WS
Robot server
Detector server
Proposal DB
•Diffraction images
•XAFS spectrum
Measurement Condition
Users lab.
Web Server D-Cha
•Diffraction images
•XAFS spectrum
Result view session
DB
Data storage
Make use of D-Cha developed for mail-in
• User info.
• Sample info.
Diffractometer & sample changer

Client GUI software

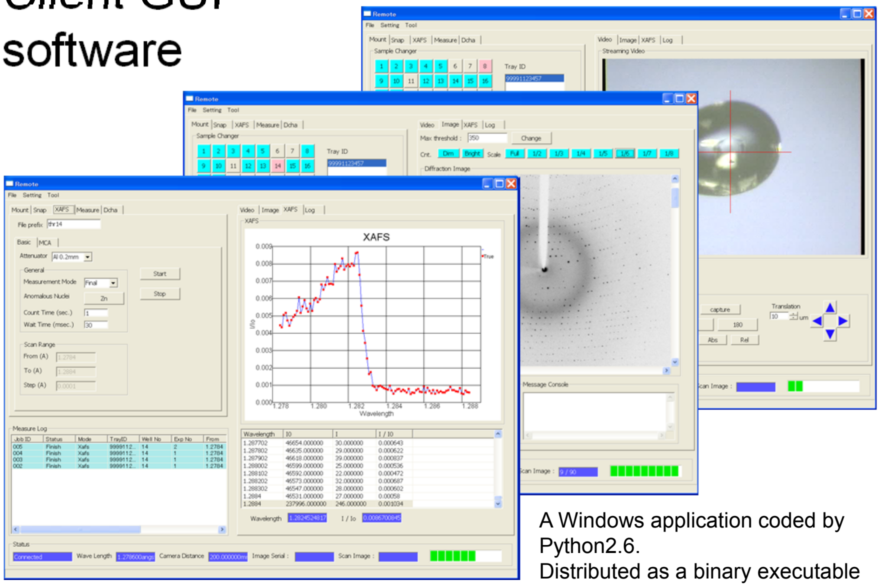

A Windows application coded by Python2.6.
Distributed as a binary executable

Radiation damage

Radiation damage

Bacterial flagelin F41 Crystal
@ SPring-8 BL41XU

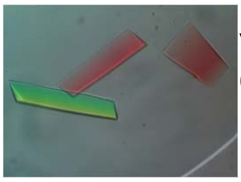

Very Thin Crystal (≒10μm)

1st frame ***15min.*** ***25min.***

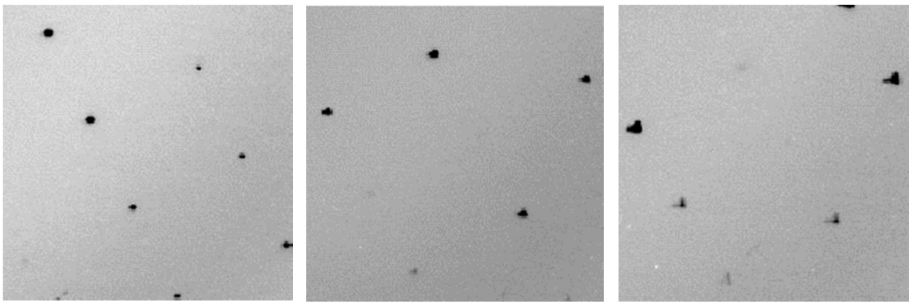

Total Flux at Sample **≒ 10^{13} photons/sec/mm^2**

F.A. Samatey, K.Imada, S.Nagashima, K.Namba (ERATO, Osaka Univ.)

63

Interaction between photon and protein

Primary Effect

・Absorbed photon energy > **Temperature increment**
・Photoelectron formation
> **Chemical reduction / Reactive radical formation**
X-ray dose dependent
Temperature / Time independent

Secondary Effect

・Chemical reaction by free radicals

X-ray dose, temperature / time dependent

64

Photon-electron interaction

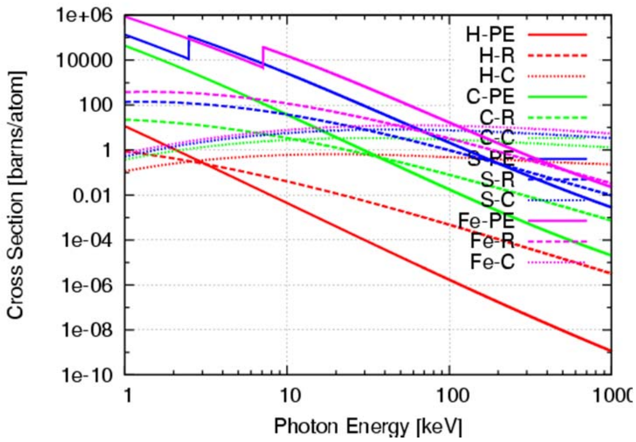

PE: Photoelectric absorption, R: Thomson (Reyleigh) scattering,
C: Compton scattering

65

Cryocrystallographic technique

Suppress thermal degradation of sample
diffusion and reaction of free radicals
at cryogenic temperature (30 – 100 K)
using cold N_2/He gas stream

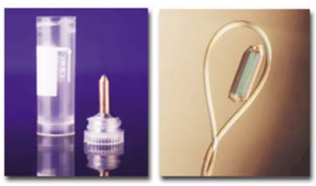

Sample Mount Pin & Cryoloop

66

Radiation induced temperature increment under cryogenic condition

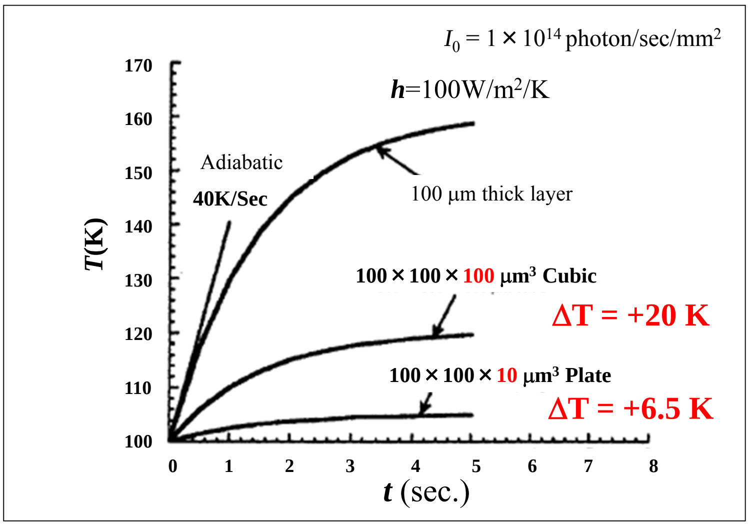

Heat transfer speed depends on crystalline size and shape.

Kuzay *et al.* Acta Cryst. (2001). D57, 69-81

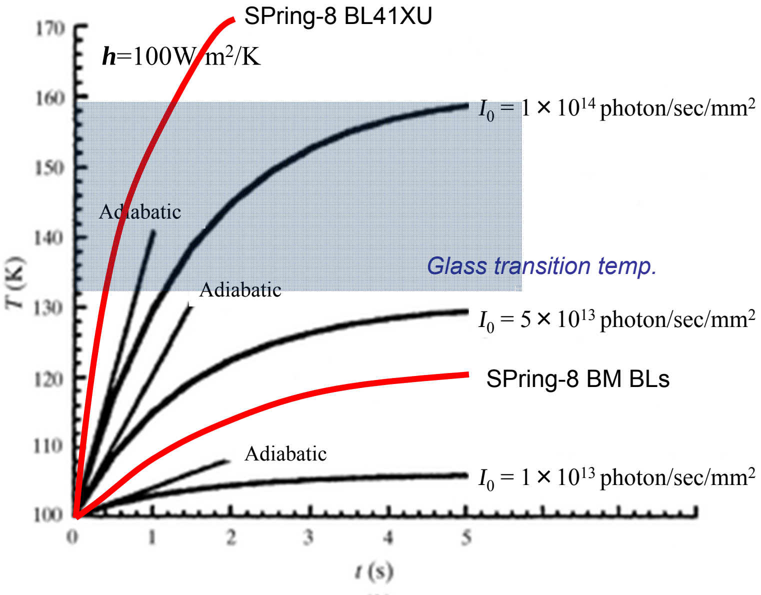

Kuzay *et al.* Acta Cryst. (2001). D57, 69-81

Phase transition of water

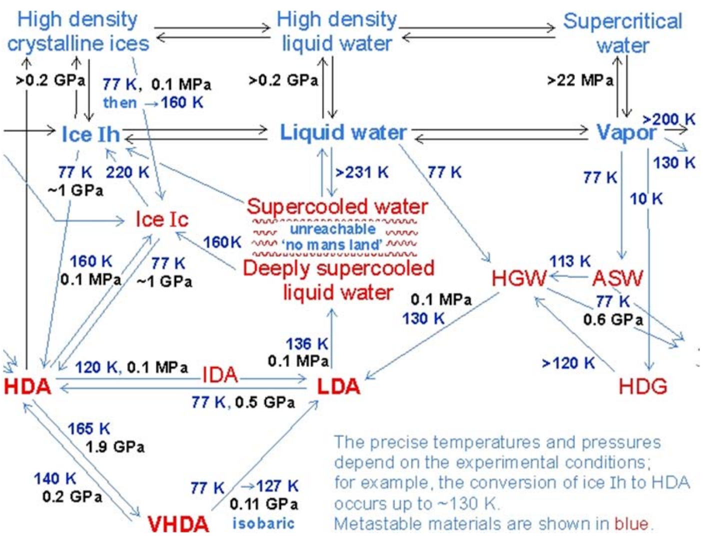

Water structure and science *by Martin Chaplin*
http://www.btinternet.com/~martin.chaplin/

69

Reactive radical formation by photoelectron production

Water

	$h\nu$	
H_2O	$\longrightarrow$	$H_2O^+ + e^-$
$H_2O^+ + H_2O$	$\longrightarrow$	$H^+ + OH\cdot$
$e^- + H_2O$	$\longrightarrow$	H_2O^-
$H_2O^- + H_2O$	$\longrightarrow$	$H\cdot + OH^-$
H_2O	$\longrightarrow$	$H\cdot + OH\cdot$

Hydroxyl radical
Half-life ~10^{-9} s

Disulfide bridge	
(p)-CH_2SSCH_2-(p)	(p)-$CH_2SS\cdot^+CH_2$-(p) + e^-
(p)-CH_2SSCH_2-(p) + $OH\cdot$	(p)-$CH_2SS\cdot^+CH_2$-(p) + OH^-
(p)-$CH_2SS\cdot^+CH_2$-(p) + OH^-	(p)-CH_2SOH + (p)-$CH_2S\cdot$
(p)-CH_2SSCH_2-(p) + $OH\cdot$	(p)-CH_2SOH + (p)-$CH_2S\cdot$
Cysteine	
(p)-CH_2SH + e^-	(p)-CH_2 + SH^-
(p)-CH_2SH + H	(p)-CH_2 + H_2S
Aspartate & Glutamate	
(p)-CH_2CH_2COO-	(p)-$CH_2C\cdot^+H_2COO$- + e-
(p)-$CH_2C\cdot^+H_2COO$-	(p)-$CH_2CH_2\cdot$ + CO2
Tyrosine	
(p)-$CH_2C_6H_4OH$	(p)-$CH_2C_6H_4OH\cdot$+ + e-
(p)-$CH_2C_6H_4OH\cdot^+$	(p)-$CH_2C_6H_4O\cdot$ + H+
Methionine	
(p)-$CH_2CH_2SCH_3$ + $2H\cdot$	(p)-CH_2CH_3 + CH_3SH

70

Burmeister, Acta Cryst. (2000). D56, 328-341

Estimation of radiation damage

Sample	Hen egg white lysozyme	
Space group	$P4_32_12$	
Lattice	a = 78.54 , c = 37.77 Å	

BL	SR (SPring-8 BL45XU)	
Data set	11(1 ~ 11)	1 (12)
image/set	95	245
Wavelength	1.02Å	1.02Å
Oscillation angle	1.0°	1.0°
Camera distance	150mm	220mm
Exposure	5 sec	60 sec
Detector	Jupiter210(CCD)	RAXIS-V (IP)

71

N. Shimizu (JASRI) et al.

Variation of I/σ_I and R_{merge}

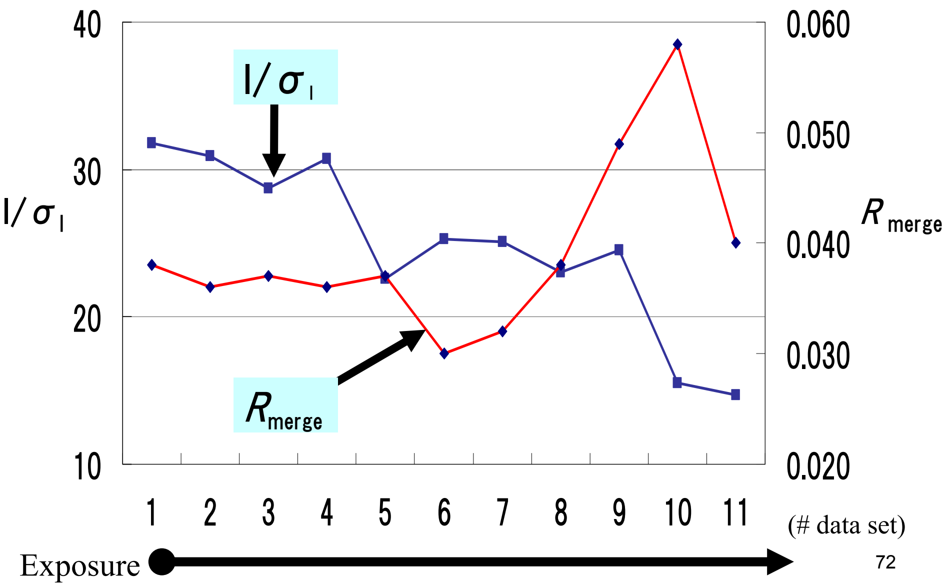

72

Variation of lattice constants

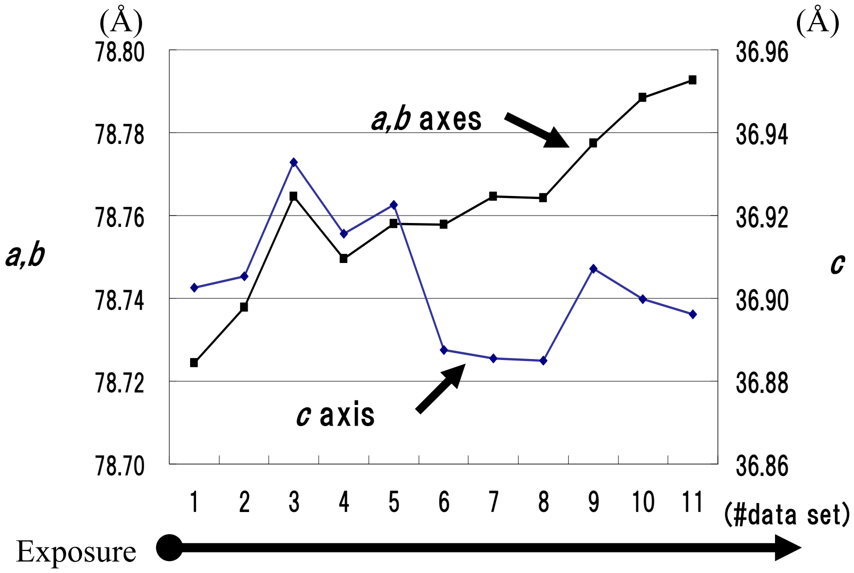

73

Radiation damage in real space

electron density at 1.6 Å resolution

Data set

1

R-factor 18.51 %
R *free* 20.64 %

fo-fc 2.5σ
fo-fc −2.5σ
2fo-fc 1.0σ

12

R-factor 18.50 %
R *free* 20.68 %

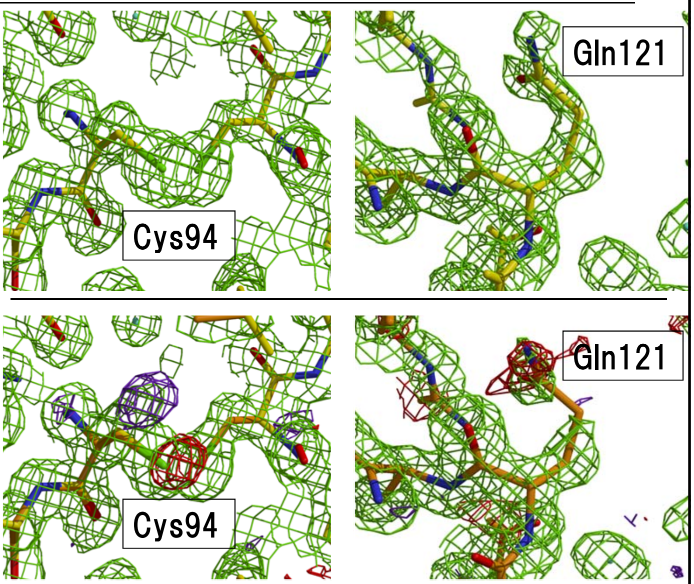

Dose limit

Estimated dose limit for ionizing radiation

3×10^{17} **keV/mm^3 (~ 5×10^7 Gy)**

1×10^{16} **$photon/mm^2$ @ 12.4keV**

(Henderson, R. (1990). *Proc. R. Soc. London Ser. B*, **241**, 6-8.)

4×10^{17} **keV/mm^3**

(Gonzalez, A., Nave, C. (1994). *Acta Cryst. D* **50**, 874-877.)

5×10^{16} **$photon/mm^2$ @ 12.4keV**

(Sliz, P.,Harrison,S.C.Rosenbaum,G., (2002). *Structure*, **11**, 13-19.)

75

How to mitigate & manage the radiation damage ?

- Use of a helium gas cryostream lowers the sample temperature to around 35 K.

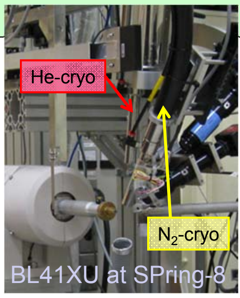

- Many works reported the effect of the low temperature below 100K.
- The behavior of the generated hydrogen gas changes depending on the temperature?

(Alke Meants, RD5 (2008), PSI)

- Use of as high X-ray energy as possible.

The damage is generally thought to decrease at higher X-ray energy as the absorption is lower.

- Dose control

Dose Calculation (*RADDOSE**)

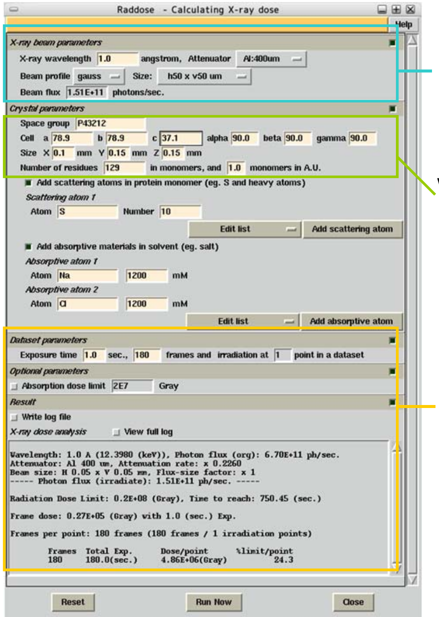

*Raddose** GUI for SPring-8 BL (Kawamoto (JASRI) et al.)

- Beam size and thickness of the attenuator are chosen from a pull down menu.
- Photon flux (PHOSEC) is automatically calculated by parameter tables of the flux, the beam size and the attenuator against wavelength.
- Although the number of monomers in the asymmetric unit is inputted, it is changed into the number of monomers in the unit cell (NMON) by using CCP4 libraries.
- As for the percentage for dose limit, the value per a irradiation point is displayed.
- The original log file of RADDOSE is displayed when "View full log" is checked.

*) Murray, J. W. et al. (2004). *J. Appl. Cryst.*, **37**, 513-522.

In case of a membrane protein: Ca^{2+}-ATPase in various states

$E1 \cdot 2Ca^{2+}$	E1·ATP (AMPPCP)	E1P·ADP ($AlF_4^- \cdot$ADP)	E2·Pi (MgF_4^{2-})	E2 (TG,BHQ,CPA)

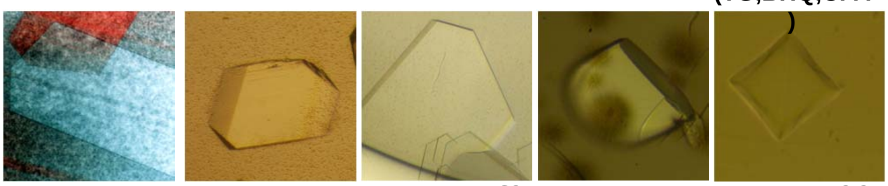

C2 1.95 Å	C2 2.5 Å	C2 2.4 Å	$P2_1$ 2.3 Å	$P4_12_12$ 2.1 Å

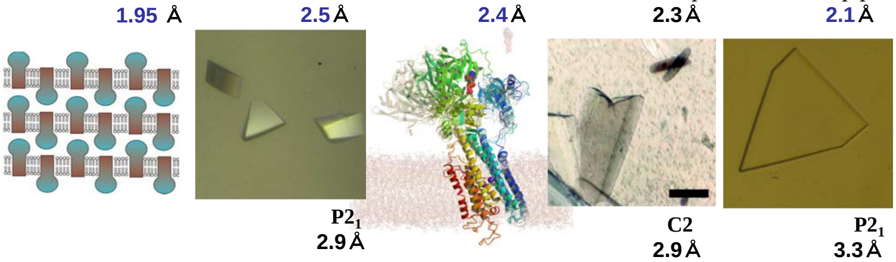

	$P2_1$ 2.9 Å		C2 2.9 Å	$P2_1$ 3.3 Å

78

Courtesy of Prof. C. Toyoshima (Univ. Tokyo)

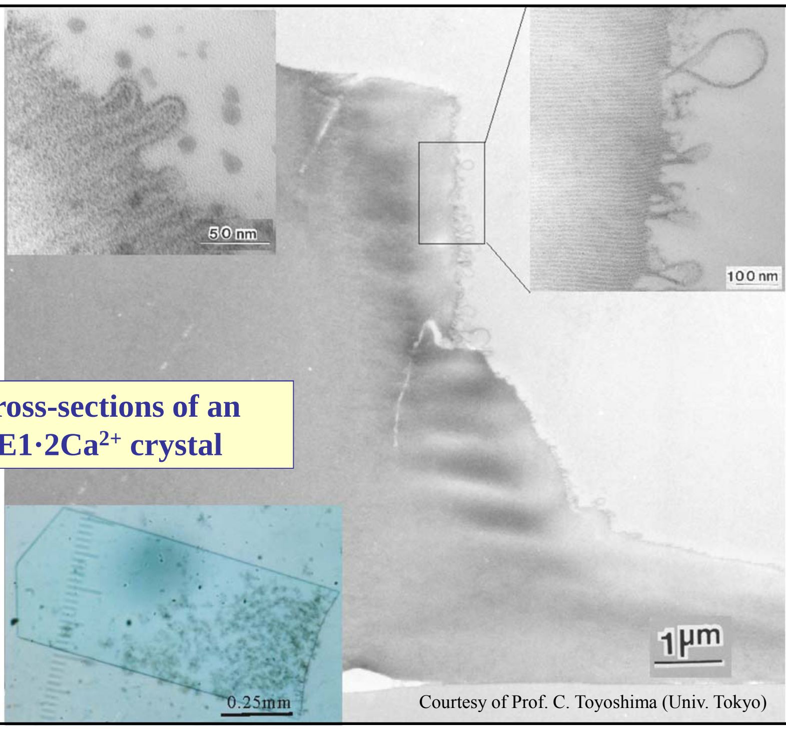

cross-sections of an E1·2Ca^{2+} crystal

Courtesy of Prof. C. Toyoshima (Univ. Tokyo)

79

Data acquisition tools

Multiple X-ray exposures on one/several crystals
to control serious radiation damage during data collection
to find better diffracting crystals or crystal segments

･Vector Centering :

Changing exposure position linearly in every constant frames on *One crystal*

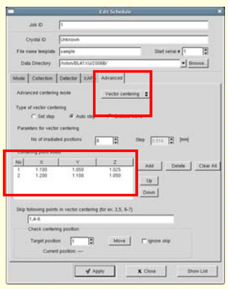

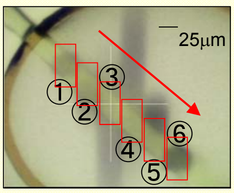

･Multiple Centering :

Multiple exposure positions using several crystals in *One cryo-loop*

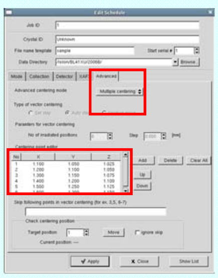

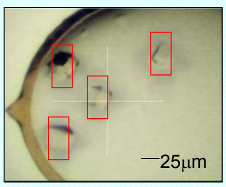

80

Anomalous data collection

81

Harker Diagram ~ Structure factor and phase

$$\mathbf{F}(\mathbf{h}) = |\mathbf{F}(\mathbf{h})| \exp i\alpha$$
$$= \sum f_j \exp 2\pi i \mathbf{h} \cdot \mathbf{r}_j$$

Complex space

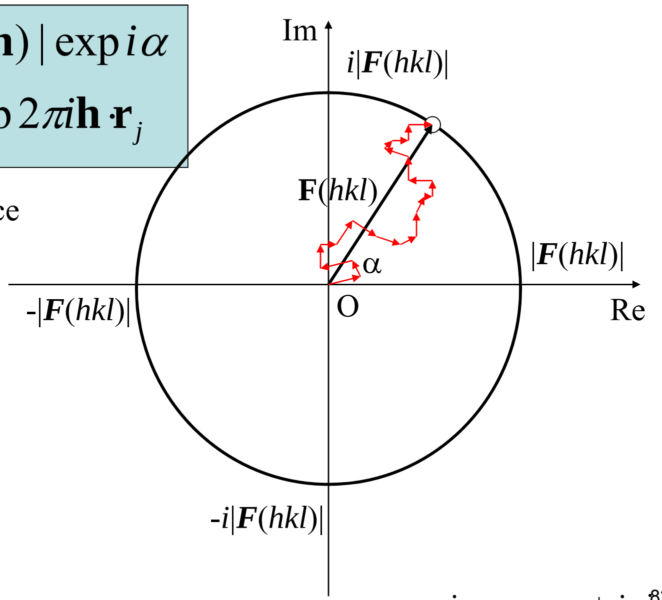

exp iα = cos α + i sin α

82

Isomorphous replacement

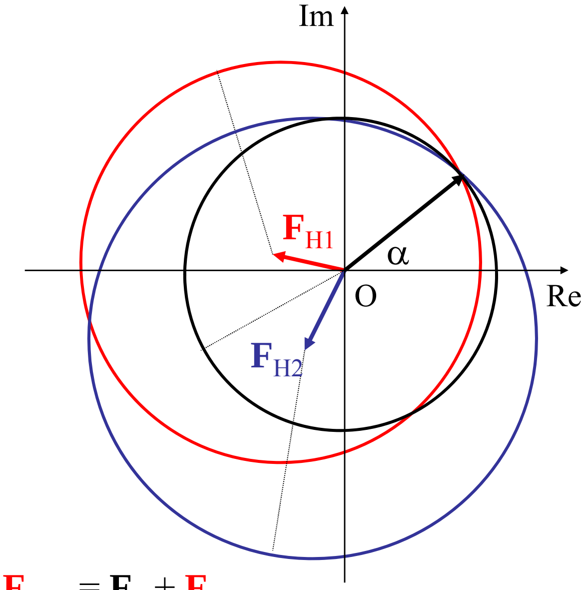

$|\mathbf{F}_P|$: Native

$|\mathbf{F}_{PH1}|$: Derivative 1

$|\mathbf{F}_{PH2}|$: Derivative 2

$\mathbf{F}_P = |F_P| \exp i\alpha$

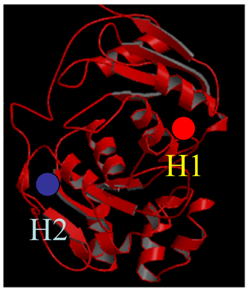

$\mathbf{F}_{PH1} = \mathbf{F}_P + \mathbf{F}_{H1}$

83

Anomalous Phasing

Anomalous Effect

Anomalous term of zinc (Z_e = 32)

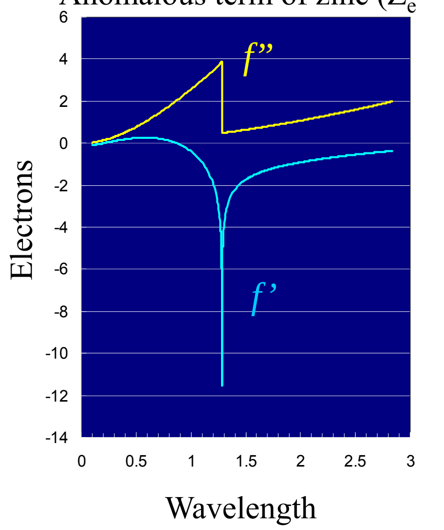

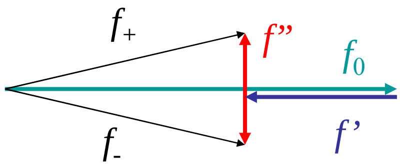

$f_\pm = f_0 + f' \pm i f''$

Smaller than usual heavy atom effects

↓

Need high quality data

84

2 Wavelength MAD

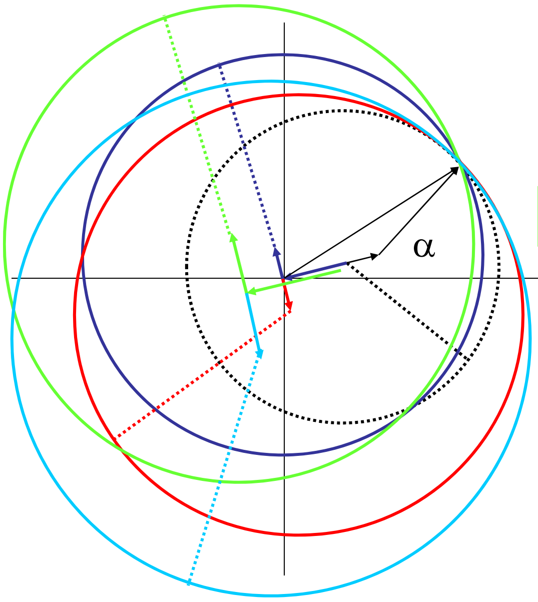

$|F|$: Native

$|F_{\lambda 1}(\mathbf{h+})|$: Anomalous

$|F_{\lambda 1}(\mathbf{h-})|$: Anomalous

$|F_{\lambda 2}(\mathbf{h+})|$: Anomalous

$|F_{\lambda 2}(\mathbf{h-})|$: Anomalous

$\mathbf{F}_P = |F_P| \exp i\alpha$

Single phase solution
can be determined.

85

Incident wavelength and anomalous signal

Oxidation state and XANES spectra for Se

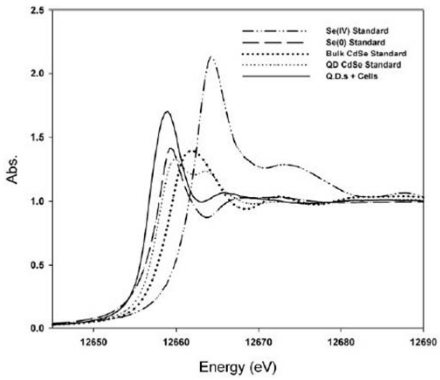

Holden & Nadeau, 2008

Anisotropic anomalous scattering factors f′ and f″ for Se in SeMet

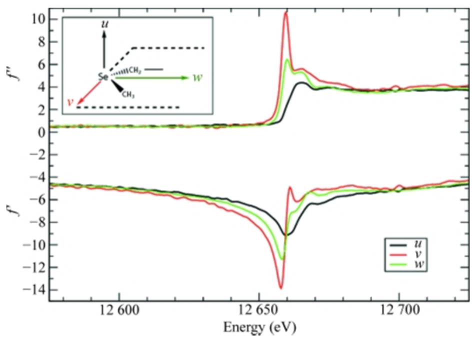

Schiltz & Bricogne, Acta Cryst D64, 711 (2008)

86

Recent trend of isomorphous phasing

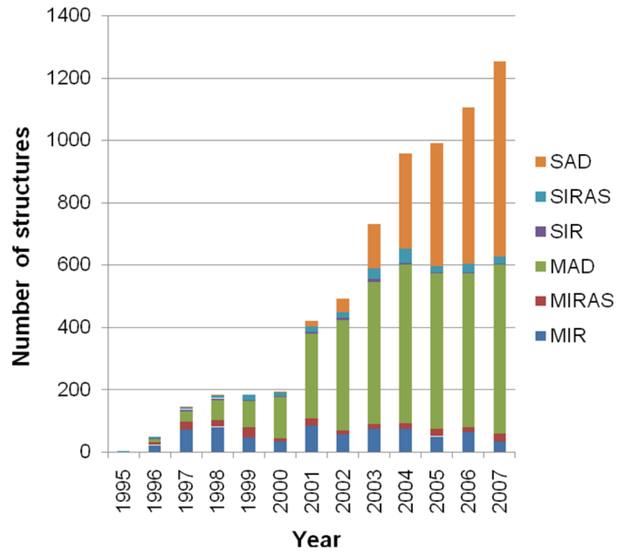

87

SAD

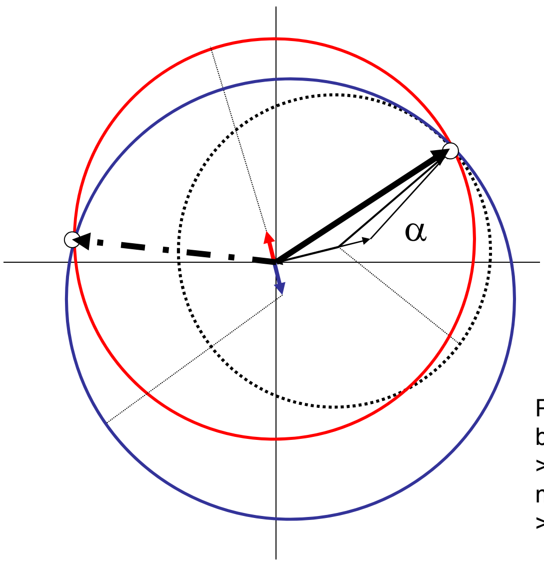

| F |: Native

| F_λ (**h+**) | : Anomalous

| F_λ (**h−**) | : Anomalous

Phase probability function shows bimodal.
>> Phase improvement by density modification
>> High precision data collection

88

Estimation of anomalous signal

- Anomalous signal indicator
  - Bijvoet difference
    $\langle|\Delta F^{\pm}|\rangle / \langle|F|\rangle = \sqrt{2N_A/N_P} / \left(f'' / f^0_{\text{eff}}(\theta)\right)$
  - *R*anom, *R*anom/*R*pim
  - Anomalous SN ratio $\langle \Delta F^{\pm} / \sigma(\Delta F^{\pm}) \rangle$

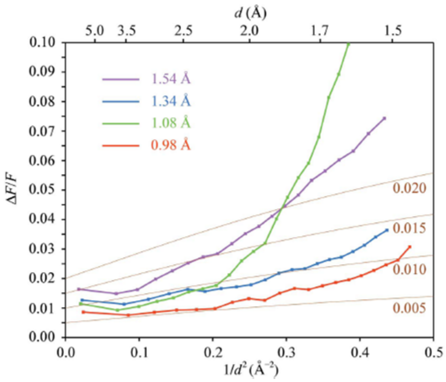

89

Dauter, Acta Cryst. D62, 867 (2006).

Phasing power ~ NCS / %Solv

%Solv

#NCS	10	20	30	40	50	60	70	80	90
1	1.11	1.25	1.43	1.67	2.00	2.50	3.33	5.00	10.00
2	1.57	1.77	2.02	2.36	2.83	3.54	4.71	7.07	14.14
3	1.92	2.17	2.47	2.89	3.46	4.33	5.77	8.66	17.32
4	2.22	2.50	2.86	3.33	4.00	5.00	6.67	10.00	20.00
5	2.48	2.80	3.19	3.73	4.47	5.59	7.45	11.18	22.36
6	2.72	3.06	3.50	4.08	4.90	6.12	8.16	12.25	24.49
7	2.94	3.31	3.78	4.41	5.29	6.61	8.82	13.23	26.46
8	3.14	3.54	4.04	4.71	5.66	7.07	9.43	14.14	28.28
9	3.33	3.75	4.29	5.00	6.00	7.50	10.00	15.00	30.00
10	3.51	3.95	4.52	5.27	6.32	7.91	10.54	15.81	31.62
15	4.30	4.84	5.53	6.45	7.75	9.68	12.91	19.36	38.73
20	4.97	5.59	6.39	7.45	8.94	11.18	14.91	22.36	44.72
25	5.56	6.25	7.14	8.33	10.00	12.50	16.67	25.00	50.00

Arnold & Rossmann, *PNAS* 83, 5489-5493 (1986)

90

S-SAD Phasing of Thaumatin

Thaumatin (miracle fruit)	
Mol. weight	22.132 Da
Amino Acids	206 residues
Sulfurs	Met : 1 Cys : 16 (S-S : 8) 12.1 res. / 1 Sulfur
Space group	$P4_12_12$
Solv. Content	0.54

Experimental conditions

Crystal size	0.20 mm x 0.10 mm x 0.05 mm
Beam size	0.05 mm x 0.05 mm
Exposure	1 sec. exposure, 1deg. oscillation, 360 frames

Software

HKL2000(+SCALA)+ SHELX C/D + SOLVE/RESOLVE + ARP/wARP

M. Kawamoto (JASRI, SagaLS) et al.

S-SAD Phasing of Thaumatin

λ	1.10 Å	1.30 Å	1.50 Å	1.70 Å	1.90 Å
Distancce	150 mm	150 mm	110 mm	110 mm	110 mm
Cell	a = 57.873, c = 150.186 Å	a = 57.821, c = 150.142 Å	a = 57.985, c = 150.393 Å	a = 57.895, c = 150.247 Å	a = 57.845, c = 150.137 Å
Resolution			50 – 2.1 Å		
0 – 45º (multi.≒1.9)					0.032 / 0.046 (0.051) 0 -
0 – 60º (multi.≒2.5)					0.026 / 0.038 (0.049) 13 4 % (0.303 / 0.624)
0 – 90º (multi.≒3.8)				0.018 / 0.023 (0.037) 0 -	
0 – 120º (multi.≒5)			0.014 / 0.020 (0.040) 0 -	0.016 / 0.022 (0.043) 11 40 % (0.303 / 0.612)	0.020 / 0.028 (0.055) 12 4 % (0.299 / 0.588)
0 – 180º (multi.≒7.5)			0.013 / 0.017 (0.043) 13 27 % (0.305 / 0.575)	0.015 / 0.020 (0.051) 10 94 %(0.280 / 0.365)	0.019 / 0.025 (0.063) 12 99 % (0.208 / 0.257)
0 – 240º (multi.≒10)		0.012 / 0.019 (0.059) 0 -	0.011 / 0.015 (0.044) 14 99 % (0.222 / 0.280)		
0 – 360º (multi.≒15)	0.009 / 0.013 (0.047) 0 -	0.011 / 0.017 (0.060) 11 41 % (0.305 / 0.562)	0.010 / 0.014 (0.051) 15 99 % (0.227 / 0.299)	0.013 / 0.015 (0.057) 12 99 % (0.206 / 0.222)	0.016 / 0.019 (0.071) 14 99 % (0.192 / 0.243)

R_{anom} / R_{pim} (R_{merge})
found sulfurs
Seq. Cov. (R_{work}/R_{free})

- **Model constructed**
- **Model constructed in part**
- **Substructure determined**
- **No solution**

M. Kawamoto (JASRI, SagaLS) et al.

S-SAD phasing of Lysozyme @ SPring-8 BM BL

- Mw 14,307 Da
  129 residues
- Sulfurs Met: 2
  Cys: 8 (S-S: 4)
  12.9 res./1 sulfer
- %Solv 0.37

・Resolution (Å)	50.00-1.08 (1.12-1.08)
・Space group	$P4_32_12$
・Unit cell (Å)	a = 78.88, c =36.93
・Redundancy	26.4(11.9)
・Observations	2432608
・Unique reflections	46104
・Completeness (%)	96.4 (79.2)
・Rsym (%)	2.4 (36.2)
・$I/\sigma(I)$	95.56 (8.88)

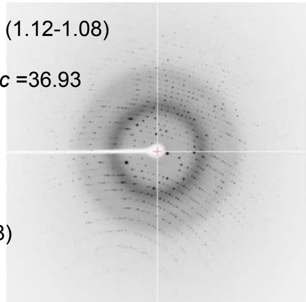

・Crystal size (um)	200 x 180x 100 [3]
・Wavelength (A)	0.85 Å
・Oscillation range	720 deg.
・Oscillation angle	0.5 deg.
・Exposure time	1.5 sec
・Camera distance	120 mm
・Data processing	HKL2000
・Phasing	SHELXC/D/E
・Model Building	ARP/wARP

Anomalous scattering factor of sulfur

λ(Å)	f'	f"
5.01	-7.4614	4.1039
2.50	0.3564	1.3314
1.50	0.3115	0.5298
1.30	0.2689	0.4047
1.00	0.2206	0.2937
0.85	0.1509	0.1771

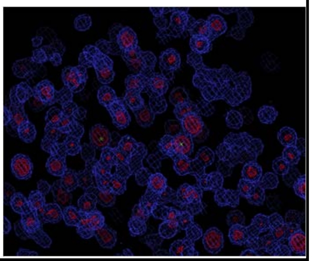

S. Baba (JASRI) et al. @ BL38B1

Damage control in MAD data collection

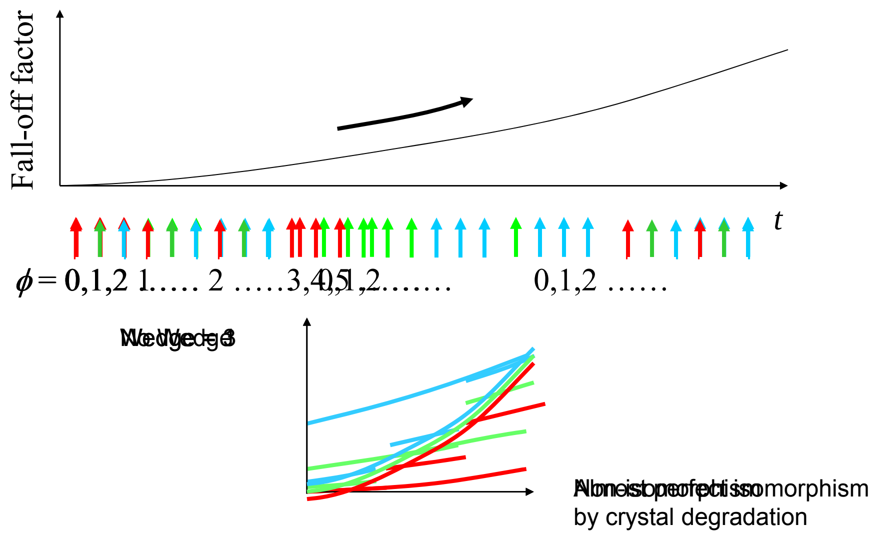

94

Overview of Beamline BL45XU

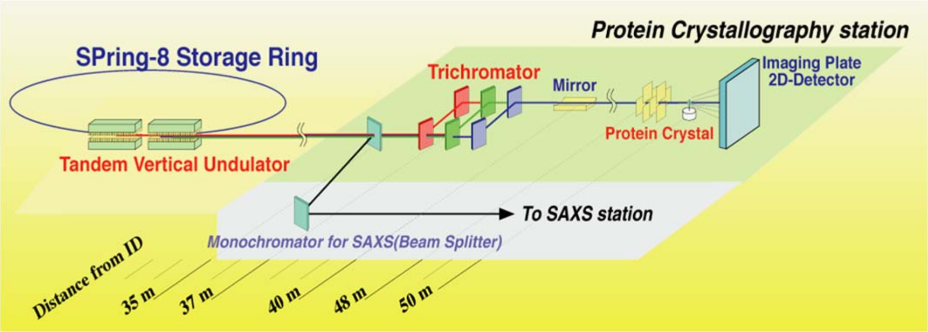

Trichromatic concept for optimizing MAD-experiment

- **Tandem vertical undulator (for High Quality Beam)**
- **Trichromator (for Rapid Data Collection)**

Yamamoto, Kumasaka, Fujisawa, Ueki (RIKEN) (1996)

95

Trichromatic Concept for MAD-experiment

Three-wavelengths data will be taken simultaneously for **the identical protein crystal** without changing the setting by **"Trichromator"**.

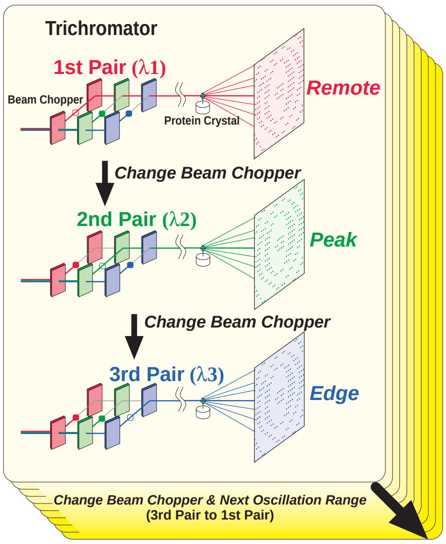

To improve MAD data,
inverse beam is also applicable.

96

Bacterial Chitosanase (Mw 34k, 7 SeMet)

Source: Gram-Negative Bacterium (*Matsuebacter chitosanotabidus* 3001)
Function: Hydrolysis of glycosidic bonds of chitosan
(○GlcN-GlcN, GlcN-GlcNAc, GlcNAc-GlcN, ×GlcNAc-GlcNAc)

$P2_12_12_1$
a = 51.5, b = 56.2, c = 206.8 Å
1.7 Å Resolution
Two monomers / Asym. unit

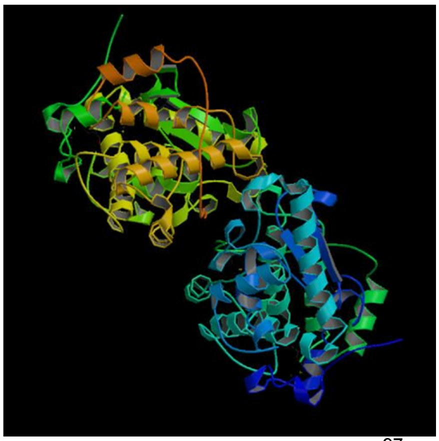

97

Kumasaka (RIKEN) *et al.*, 2002

Effect of Trichromatic Data Collection

Data Collection Statistics

Data	Observations	Individuals	I / σ	R_{merge}	R_{iso}	B
Cho1: Remote	260,402	65,579	18.5	0.049	—	—
Peak	269,821	66,482	17.4	0.053	0.057	0.08
Edge	269,362	66,428	17.5	0.084	0.048	0.11
Cho2: Remote	261,577	65,695	19.8	0.045	—	—
Peak	263,567	66,480	18.7	0.048	0.064	0.09
Edge	263,387	66,449	17.1	0.076	0.078	-0.39

Cho1 (Trichromatic)

Cho2 (Conventional)

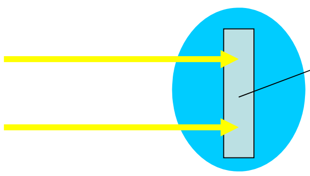

Chitosanase Crystal
(Length=0.4 μm)

98

Effect of Trichromatic Data Collection

Variation of Fall-off factor

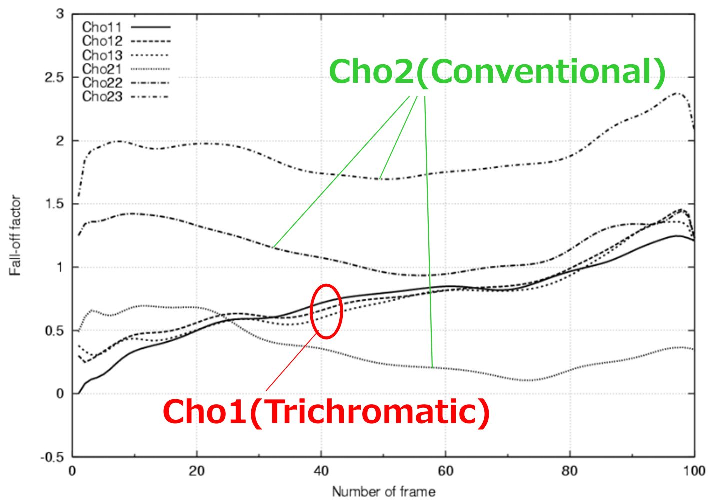

99

Effect of Trichromatic Data Collection

Comparison with dispersive Patterson maps

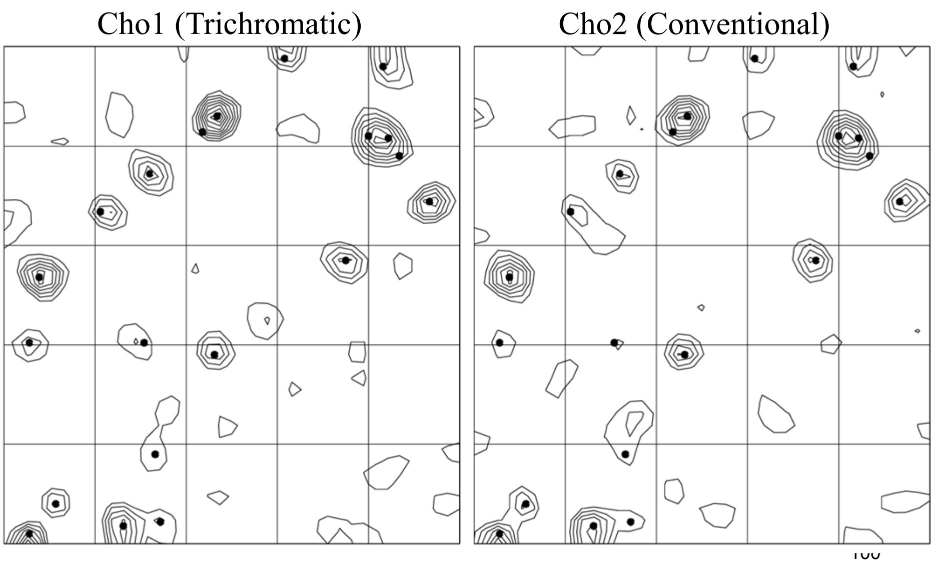

Harker section ($w = \frac{1}{2}$)

Effect of Trichromatic Data Collection

Phasing Statistics (20 – 1.7 Å)

Data	Cho1 (Trichromatic)			Cho2 (Conventional)		
	Remote	Peak	Edge	Remote	Peak	Edge
R_{Cullis} (iso)#		0.82 / 0.84	0.83 / 0.88		0.78 / 0.83	0.76 / 0.86
R_{Cullis} (ano)	0.94	0.91	0.99	0.94	0.91	0.99
Lack of closure (iso)#		8.9 / 14.0	8.1 / 12.5		11.4 / 14.7	10.3 / 16.8
Lack of closure (ano)	8.98	16.56	7.32	8.11	15.91	6.37
Figure of merit	0.6057			0.6167		
Phasing power#		1.22 / 0.81	1.19 / 0.82		1.40 / 0.90	1.38 / 0.89
$<\|\Delta\phi\|>$*	44.2	(33.9)		47.8	(39.4)	

#: Acentric and centric values before and after slash.
*: Phase difference against phases calculated from refined model
Parenthesis show the values within the range of 10-2.5 Å. 101

Effect of Trichromatic Data Collection

Phase difference against true phase

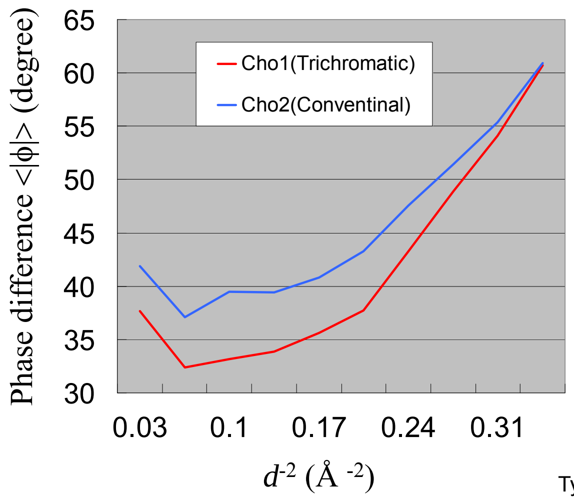

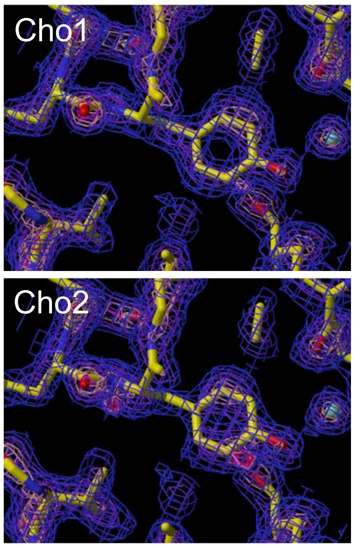

Tyr 165 (Chitosanase A-chain)
1.7 Å MAD phase 102
(without any phase modification)

Other phasing method: Molecular replacement

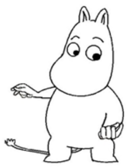

Known determined structure

Unknown
but probably similar
structure

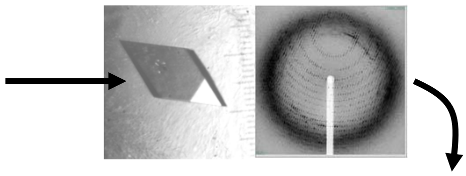

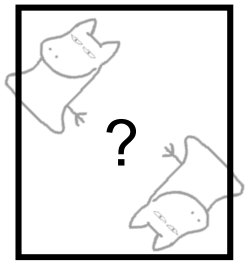

To solve unknown structure, a known structure is used as a approximation.

The known structure will be selected by sequence similarity. Highest sequence similarity might gives highest structural similarity.

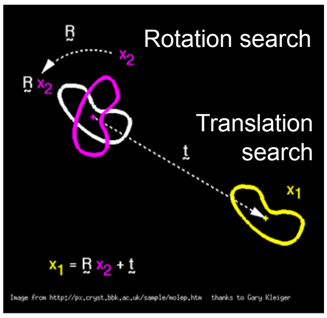

How to pack the molecules into the cell ?
> 6-D search

103

Patterson function

Intramolecular・Intermolecular vectors

Real space

$$\rho(\mathbf{r}) = \int_S \boldsymbol{F}(\mathbf{S}) \exp[-2\pi i\, \mathbf{S}\cdot\mathbf{r}]\, d\mathbf{S}$$

$$P(\mathbf{u}) = \int_S |\boldsymbol{F}(\mathbf{S})|^2 \exp[-2\pi i\, \mathbf{S}\cdot\mathbf{u}]\, d\mathbf{S}$$

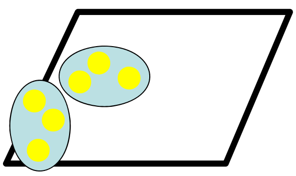

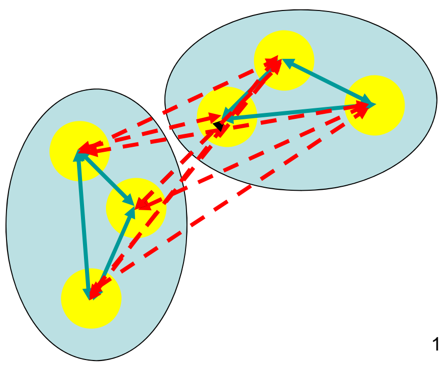

Patterson space

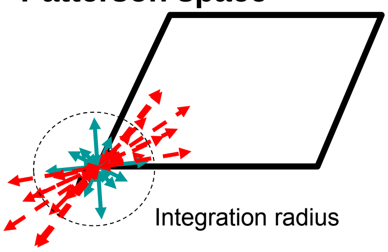

104

Euler angles, α β γ

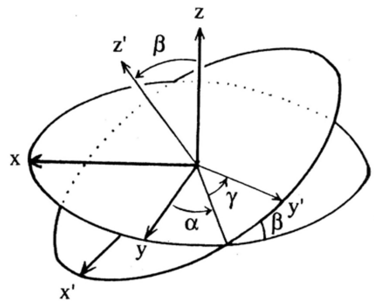

Rotation axis: z'' x' z

$$\begin{pmatrix} \cos\gamma & -\sin\gamma & 0 \\ \sin\gamma & \cos\gamma & 0 \\ 0 & 0 & 1 \end{pmatrix}\begin{pmatrix} 1 & 0 & 0 \\ 0 & \cos\beta & -\sin\beta \\ 0 & \sin\beta & \cos\beta \end{pmatrix}\begin{pmatrix} \cos\alpha & -\sin\alpha & 0 \\ \sin\alpha & \cos\alpha & 0 \\ 0 & 0 & 1 \end{pmatrix}$$

Order
in 3 step rotation: 3 2 1

105

Polar angles, φψκ

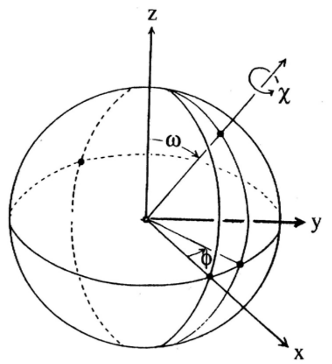

$$\begin{array}{ccccc} z'''' & y''' & z'' & -y' & -z \\ \begin{pmatrix} \cos\phi & -\sin\phi & 0 \\ \sin\phi & \cos\phi & 0 \\ 0 & 0 & 1 \end{pmatrix} & \begin{pmatrix} \cos\varphi & 0 & -\sin\varphi \\ 0 & 1 & 0 \\ \sin\varphi & 0 & \cos\varphi \end{pmatrix} & \begin{pmatrix} \cos\kappa & -\sin\kappa & 0 \\ \sin\kappa & \cos\kappa & 0 \\ 0 & 0 & 1 \end{pmatrix} & \begin{pmatrix} \cos\varphi & 0 & \sin\varphi \\ 0 & 1 & 0 \\ -\sin\varphi & 0 & \cos\varphi \end{pmatrix} & \begin{pmatrix} \cos\phi & \sin\phi & 0 \\ -\sin\phi & \cos\phi & 0 \\ 0 & 0 & 1 \end{pmatrix} \\ 5 & 4 & 3 & 2 & 1 \end{array}$$

Real rotation ~ κ

106

An example of rotation function

α	β	γ	x	y	z	Correlation Coefficient	R-factor
30.37	54.61	351.97	0.000	0.000	0.000	16.0	48.9
59.63	125.39	171.97	0.000	0.000	0.000	16.0	48.9
27.57	41.41	20.51	0.000	0.000	0.000	9.2	51.1
62.43	138.59	200.51	0.000	0.000	0.000	9.2	51.1
17.43	98.67	334.32	0.000	0.000	0.000	7.2	51.7
72.57	81.33	154.32	0.000	0.000	0.000	7.2	51.7
41.73	139.11	197.95	0.000	0.000	0.000	7.7	52.1
48.27	40.89	17.95	0.000	0.000	0.000	7.7	52.1
81.84	98.18	226.67	0.000	0.000	0.000	8.2	51.6
8.16	81.82	46.67	0.000	0.000	0.000	8.2	51.6

Modeling & refinement of structure

Modeling: Construct molecular model to fit obtained electron density using interactive molecular graphics software or automated modeling software.

Refinement: Optimization of observed and calculated F data by shifting atomic coordinates.

R-factor: Crystallographic Reliability-factor

$$R1=\Sigma\ ||Fo|-|Fc(\mathbf{r})||/\Sigma\ |Fo|$$

$$wR2=(\Sigma\ w(|Fo|^2-|Fc(\mathbf{r})|^2)^2/\Sigma\ w(|Fo|^2)^2)^{1/2}$$

Cross validation of R-factor (R_{free})

Refinement of structural model

1) Unrestraint refinement
   - Only using R-factor refinement
   - in case of ultra-high resolutions (0.8 A or higher)

2) Restraint refinement
   - Coupled with molecular mechanics
   - Model validity is also guaranteed by low energy ~ structural stability

Target function

$$E = E_{\mathrm{chem}} + w_{\mathrm{xray}} E_{\mathrm{xray}}$$

$$E_{\mathrm{xray}} = \sum_{\mathbf{h}} \left| F_{\mathrm{O}}(\mathbf{h}) - kF_{\mathrm{C}}(\mathbf{h}) \right|^2$$

Basics of molecular mechanics (MM)

Energy calculation of atomic bonds and interactions by classical mechanics.

bond length
bond angle
dihedral/torsion
improper dihedral
van der Waals
electrostatic

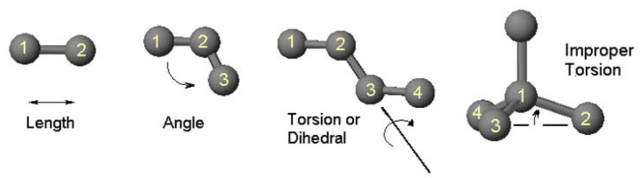

$$E_{\mathrm{chem}} = E_{\mathrm{bond}} + E_{\mathrm{angle}} + E_{\mathrm{dihe}} + E_{\mathrm{impr}} + E_{\mathrm{vdW}} + E_{\mathrm{elec}}$$

e.x. Water

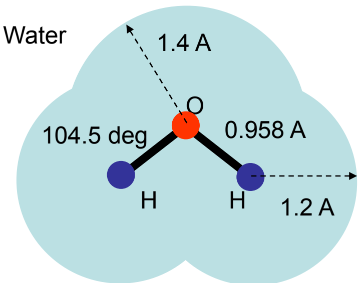

$$E_{\mathrm{bond}} = k_{\mathrm{bond}} (r - r_{\mathrm{ide}})^2$$
$$E_{\mathrm{angle}} = k_{\mathrm{angle}} (\theta - \theta_{\mathrm{ide}})^2$$

Force Field

TIPS3P Parameter

Bond O-H	450.0	0.9572
Bond H-H	0.0	1.5139
Angle H-O-H	55.0	104.52

Summary

- Signal enhancement / Noise reduction
  - Diffraction signal:
    Crystal size, Beam flux/flux density, …
  - Scattering noise
    Beam size / profile, Cryosolvent, Wavelength,
    Oscillation angle, Beam stop / Helium path, …
  - Radiation damage:
    Helium cryo, Exposure time, Shift beam position,
    Radical scavenger, …
  - Anomalous signal
    Anomalous scatterer, Wavelength, …